The Ligand Substitution Reactions of *N*-Acetyl-Co(III) Microperoxidase-8 (NAcCoMP8): a Comparison with Aquacobalamin (vitamin B_{12a})

Sadhna Mathura, Alvaro S. de Sousa, Christopher B. Perry, Isabelle Navizet and Helder M. Marques*

Molecular Sciences Institute, School of Chemistry, University of the Witwatersrand, P.O. Wits, Johannesburg, 2050 South Africa

Abstract

N-Acetyl-Co(III) Microperoxidase-8 (NAcCoMP8), a Co(III) porphyrin-containing octapeptide and aquacobalamin (H_2OCbl^+, vitamin B_{12a}) both contain Co(III), an N-donor macrocyclic equatorial ligand (porphyrin, corrin), an imidazole derivative as one axial ligand (His, 5,6-dimethylbenzimidazole) and H_2O in the other axial coordination site. This allows for an evaluation of the effect of the equatorial macrocyclic ligand on the ligand substitution reactions of Co(III). Equilibrium constants (as log *K* values) for the coordination of anionic (CN^-, N_3^-, NO_2^-, HSO_3^-) and neutral (pyridine, N-methylimidazole, methoxylamine and hydroxylamine) ligands were determined spectrophotometrically as a function of temperature and ΔH and ΔS values are reported. The log *K* value for coordination of pyridine by H_2OCbl^+ is anomalously low and DFT calculations (M06L/SVP) show that pyridine is sterically hindered for coordinating the metal ion, resulting in a long Co–N bond and a flattened corrin ring. Anionic ligands bind more strongly to H_2OCbl^+ than to NAcCoMP8 while the converse is true for the neutral ligands. It is suggested that the higher residual charge at the metal center in the corrin (+2) compared to the porphyrin (+1) is primarily responsible. The anionic and neutral ligands behave differently. Log *K* values for coordination of the anionic ligands by both NAcCoMP8 and H_2OCbl^+ parallel the pK_a of their conjugate acid. In the case of the neutral ligands, log *K* for coordination by NAcCoMP8 correlates directly with ligand basicity but there is an inverse correlation in the case of H_2OCbl^+. Log *K* and ΔH values for the reaction with anionic ligands parallel each other in the two systems, but there appears to be an inverse correlation for the neutral ligands. DFT calculations show that the bond length between the metal and the axial ligand trans to the imidazole derivative in corrin is always longer in the corrin; however, the average difference in these bond lengths is larger for the neutral ligands than for the anions. This is attributed to the increased coulombic interaction

between the anionic ligands and the greater charge on the metal center in the corrin system. A QTAIM analysis of the electron density in these DFT models shows that electron-rich anionic ligands induce a significant covalency in their bond to Co(III) in both the corrin and the porphyrin, whereas the bonding between the metal and neutral N-donor ligands is predominantly ionic. The extent of the covalency appears to be an important factor in determining the stability of the resultant complex. The significant ellipticity of the bonds to a coordinated anion indicates the presence of some multiple bonding to Co(III). Kinetics measurements show that H_2OCbl^+ is significantly more labile towards substitution by CN^- than NAcCoMP8 (k_{25} = 240 and 103 M^{-1} s^{-1}, respectively) because of a much smaller value of $\Delta H^{\ddagger}$ value which is somewhat, but not completely, compensated for by a much more negative $\Delta S^{\ddagger}$. By contrast, the reaction of N-methylimidazole occurs faster with NAcCoMP8 than with H_2OCbl^+ due to a smaller $\Delta H^{\ddagger}$ and a somewhat larger $\Delta S^{\ddagger}$. Since the intimate mechanism is probably an interchange mechanism under dissociative activation, the kinetic results are rationalized by the extent of participation of the entering ligand in the transition state. CN^- forms a more stable complex with H_2OCbl^+ (log K > 12) than NAcCoMP8 (log K = 6.04). In its reaction with H_2OCbl^+ the transition state will occur earlier along the reaction coordinate than in its reaction with NAcCoMP8 leading to a lower $\Delta H^{\ddagger}$. The converse is true for N-methylimidazole where its greater affinity for the porphyrin than the corrin (log K = 5.70 and 4.49, respectively) makes its reaction with the former faster (k_{25} = 1300 M^{-1} s^{-1} compared to 14 M^{-1} s^{-1}). Therefore there is a correlation between the thermodynamic stability of Co(III) complexes of corrin and porphyrins and the rate of substitution of axially coordinated H_2O. The nature of the macrocycle in these Co(III) systems has a profound effect on the chemistry of the metal ion.

Keywords: Microperoxidases; cobalamins; vitamin B_{12a}; ligand substitution; DFT calculations; QTAIM calculations.

1. Introduction

As outlined in the accompanying paper [1], N-acetyl-Co(III) microperoxidase-8 (NAcCoMP8) is a Co(III)-porphyrin-containing octapeptide prepared by proteolytic digestion of cytochrome *c* and replacement of iron by cobalt in the porphyrin. At concentrations below about 4.5 μM and ionic strength μ = 0.1 M, the compound is monomeric with a Soret band at 415 nm. An increase in concentration and/or ionic strength promotes its dimerization and, at sufficiently high ionic strength (> *ca.* 1 M), further aggregation and eventual precipitation from solution. The compound retains the proximal His-18 ligand (it is protonated and displaced from the metal with a pK_a of 1.74(4)) and the other axial coordination site is occupied by a water molecule; this ionizes to the hydroxo form with a pK_a of 7.5. The similarity of the coordination environment of Co(III) in NAcCoMP8 and in aquacobalamin (vitamin B_{12a}, H_2OCbl^+) provides a unique opportunity of evaluating what effect the equatorial macrocycle (porphyrin *vs.* corrin) has on the ligand binding properties of Co(III).

The substitution of coordinated H_2O in H_2OCbl^+ by exogenous ligands, including the azoles (imidazole and its derivatives) [2], has been extensively studied (see for example [3-10]). Log *K* values for substitution of coordinated H_2O in the analogous ferric heme octa- and undecapeptides, NAcFeMP8 and NAcMP11, and in ferrous NAcFeMP8 by various ligands have been reported [11-13]. Detailed studies of the kinetics of the reaction of H_2OCbl^+ [14, 15] and Fe(III)MP8 [16] with cyanide are available. The rate constants for substitution of H_2O by CN^- in H_2OCbl^+ is 250 M^{-1} s^{-1} and 4.8×10^3 M^{-1} s^{-1} for Fe(III)MP8 in 4:1 H_2O:MeOH.

A prevailing view in the early B_{12} literature was that the ligand substitution reactions of H_2OCbl^+ proceeded through a dissociative mechanism, D, since the rate of substitution varies by at most two orders of magnitude, whereas formation constants vary by over 11 orders of magnitude, and there is a linear free energy relationship between the log of the rate constant and the log of the equilibrium constant for aquation of a wide range of cobalamin complexes [17-21]. In their detailed study of the reaction of B_{12a} with cyanide, Reenstra and Jencks [14] argued that in a coordinating solvent such as water a D mechanism is unlikely and that the intimate mechanism of the reaction is an interchange mechanism H_2OCbl^+ [14, 15] under dissociative activation, I_d; therefore there will be some nucleophilic participation by the entering ligand in the transition state. Our study of the same system [15] showed that the transition state involving CN^- is

enthalpically stabilized by 25 kJ mol^{-1} relative to that involving HCN; while it is true that many anionic ligands have very similar values of $\Delta H^{\ddagger}$ and $\Delta S^{\ddagger}$ when substituting coordinated H_2O in H_2OCbl^+ [22], CN^- and SO_3^{2-} give very different activation parameters providing convincing evidence that at least these ligands participate in the transition state. Activation parameters for the reaction with primary amines depend on the identity of the amine [23], which is inconsistent with a D mechanism. Perhaps the definitive evidence proving that the rate-determining step of the reaction cannot be unimolecular release of H_2O from the metal was provided by Stochel and van Eldik [24] who demonstrated that a plot of the observed rate constant against pyridine concentration shows saturation for [pyridine] > 0.5 M. Since a variety of ligands (hydroxylamine, imidazole, pyridine, 4-methylpyridine, methyl glycinate, histamine [25] and SCN^-, I^-, N_3^-, NO_2^-, $S_2O_3^{2-}$ [26]) saturate to very different values, the saturating rate constant cannot be that for unimolecular release of H_2O from Co(III), excluding a D mechanism. Therefore, the intimate mechanism is likely to be I_d.

We compare and contrast here the equilibrium constants for the substitution of coordinated H_2O in H_2OCbl^+ and in NAcCoMP8 by four neutral ligands, pyridine (Py), N-methylimidazole (NMI), methoxylamine (MOA) and hydroxylamine (HA)), and four anionic ligands (CN^-, N_3^-, NO_2^-, HSO_3^-). We also report the kinetics for substitution of H_2O in NAcCoMP8 by NMI and CN^-, and so evaluate the effect of the equatorial ligand on the thermodynamics and kinetics of these ligand substitution reactions.

2. Experimental

Materials were purchased from the following suppliers and used without further purification: potassium cyanide, sodium nitrite, sodium sulfite: Merck; sodium azide: Fluka; pyridine, N-methylimidazole, hydroxylamine sulfate, methoxylamine hydrochloride: Sigma-Aldrich; hydroxocobalamin: Roussel. Water was purified using a Millipore RO unit and further purified using a Millipore MilliQ unit (18 MΩ cm). UV-visible spectra were recorded in 10 mm pathlength quartz cuvettes on a Cary 1E or Cary 300 UV-visible spectrophotometer. The pH was measured using a Metrohm 720 or 827 pH meter with a Unitrode or Biotrode electrode calibrated with standard buffers.

Equilibrium constants, K, for substitution of coordinated H_2O in NAcCoMP8 and H_2OCbl^+ were determined by spectrophotometric titration usually in the temperature range 10 – 40 ^oC using appropriate buffers (μ = 0.1 M). These equilibrium constants are a function of pH because of the ionization of coordinated H_2O and, in many cases,

protonation of the ligand (Scheme 1 where N represents the proximal ligand (His in NAcCoMP8, dimethylbenzimidazole (dmbzm) in H_2OCbl^+) and the overall charge is ignored for convenience).

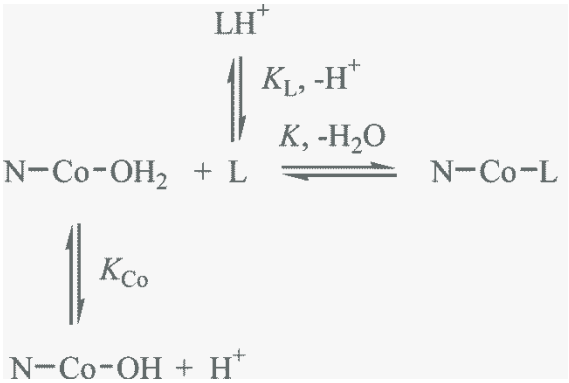

Scheme 1

As has been shown in previous studies on the ligand substitution reactions of H_2OCbl^+ [2], NAcFe(III)MP8 [11] and NAcFe(II)MP8 [27], the observed equilibrium constant, K_{obs}, which is a conditional equilibrium constant, may be converted to a pH-independent value, K (Scheme 1), by taking into account the acid dissociation constant of the entering ligand, L, and that of H_2O coordinated to Co(III), expressed as pK_L and pK_{Co}, respectively (eq. 1).

$$K = K_{obs}(1+10^{pH-pK_{Co}})(1+10^{pK_L-pH}) \quad (1)$$

Values of K_{obs} were obtained by fitting the change in absorbance as a function of ligand concentration to eq. 2 using standard non-linear least squares methods, where A_T is the absorbance at the monitoring wavelength at a particular ligand concentration [L], A_o is the absorbance before the addition of any ligand, and A_1 is the absorbance after complete replacement of coordinated H_2O.

$$A_T = \frac{A_0 + A_1 K_{obs}[L]}{1 + K_{obs}[L]} \quad (2)$$

When log K_{obs} is relatively large (*ca.* > 4), the implicit assumption in eqn. 2 that $[L]_{free} \approx [L]_{total}$ is not valid because a significant fraction of the added ligand will be complexed to the metal ion. In this case [L] in eq. 2 has to be replaced by an explicit expression for the

free ligand concentration, $[L]_{free}$. It can be shown [28] that $[L]_{free}$ is given by a quadratic expression, only one root of which has physical meaning (eq. 3), where $[M]_{total}$ is the total metal ion concentration.

$$[L]_{free} = \frac{-a_2 \pm \sqrt{a_2^2 - 4a_1a_3}}{2a_1} \qquad (3)$$
$$a_1 = K; \quad a_2 = 1 + K[M]_{total} - K[L]_{total}; \quad a_3 = -[L]_{total}$$

Because of the relatively small spectroscopic changes that occur on replacement of coordinated H_2O in NAcCoMP8, and its low concentration (ca. 1.25 μM to ensure that it is monomeric [1]), only data from the Soret region could be used. Typically, the absorbance changes 20 nm each side of the isosbestic point in the Soret region, at 1 nm intervals, were fitted to the appropriate isotherm (eqn. 2 with, or without the correction of eqn. 3, as appropriate). A weighted average of the K_{obs} values obtained at each wavelength was then determined, where the weighting factor was the reciprocal of the standard error of the fit. Using this weighted average of K_{obs} and eq. 1 leads to the average log K values reported in this work.

In the case of H_2OCbl^+, where much higher concentrations of the chromophore could be used (typically 30 μM) and where there are very significant spectroscopic changes not only in the γ band region (350 nm) but also in the $\alpha\beta$ region (470-570 nm) and sometimes in the DE region (410-430 nm), the spectroscopic changes at several wavelengths in these region were fitted, and K_{obs} values were averaged in a similar manner.

The kinetics of the substitution of coordinated H_2O in NACCoMP8 by one anionic (cyanide) and one neutral (NMI) ligand were studied as a function of temperature using conventional UV-vis spectrophotometry. The reaction of cyanide with NAcCoMP8 (concentration between 1 and 2 μM) was studied under pseudo first order conditions as a function of temperature between 15 and 35 ^oC by monitoring the decrease in absorbance at 415 nm and the increase in absorbance at 429 nm as a function of $[CN^-]$ at pH 7 (0.1 M MOPS buffer). The observed pseudo first order rate constant, k_I^{obs}, was obtained by fitting a standard exponential function to the experimental data, and corrected for the pK_a of NAcCoMP8. Between five and eight different cyanide solutions with an effective $[CN^-]$ (after correction for the pK_a of HCN) of typically between 10 and 150 μM were

used at each temperature. Cyanide solutions were used immediately after preparation. The second order rate constant, k_{II}, was obtained from the gradient of a plot of k_I against [CN^-]. The average value of k_{II} obtained at the two monitoring wavelengths was used in Eyring plots of $\ln(k_{II}h/k_BT)$ against T^{-1} to obtain the activation parameters $\Delta H^{\ddagger}$ and $\Delta S^{\ddagger}$ from the gradient and intercept, respectively.

A similar approach was used for studying the reaction of NAcCoMP8 with NMI. The maximum absorbance changes were found to occur at 413 and 424 nm (at which wavelengths the absorbance decreases and increases, respectively) and these wavelengths were used to monitor the reaction. Unfortunately, the very small absorbance changes accompanying the ligand exchange made the data quite noisy. The reactions were studied at between five and eight NMI concentrations between 3 and 35 μM (after correction for the pK_a of NMI) at pH 7 (0.1 M MOPS) with [NAcCoMP8] ca. 0.5 μM.

The reaction of H_2OCbl^+ with NMI was monitored at 351 and 360 nm, with [NMI] typically between 0.3 and 3 mM (after correction for the pK_a of NMI), [H_2OCbl^+] ca. 30 μM, pH 7 (0.1 M MOPS). The observed pseudo first order rate constants were corrected for the pK_a of H_2OCbl^+.

Computational details. DFT calculations were carried out using the Gaussian 09 [29] suite of programs. Models used for the calculation of the structure of the pyridine, imidazole and nitrite adducts of cobalamin were based on the crystal structures of NO_2Cbl [4], and $ImCbl^+$ [30] after suitable editing. For all calculations, the *b*, *d*, *e*, and *f* propionamide side chains were replaced by methyl groups, while the *a*, *c*, and *g* acetamide groups were left in place. The *α*-axial ligand was truncated at the N_γ–C bond to just include dmbzm. Since no crystal structure of PyCbl is available, the model system was based on the crystal structure of $ImCbl^+$, constructed by removing the imidazole ligand and replacing it with pyridine. The pyridine ligand was positioned such that its orientation relative to the corrin ring was the same as that for imidazole. To compare the bonding of the same ligands in porphyrin and corrin, models were constructed with all side chains of the two macrocycles replaced by H, imidazole as the lower axial ligand, and NH_3, NH_2OH, NH_2OMe, Imidazole, CN^-, NO_2^-, HSO_3^- and N_3^- as the *trans* axial ligand. Geometry optimizations were performed using the M06L density functional [31], and the SVP [32] basis set in combination with the SVP density fitting basis set [33, 34] (M06L was chosen to allow us to take advantage of the performance gains afforded by using the density fitting approximation [35, 36]). The topological properties of the electron density (ρ) were analyzed using Bader's Quantum Theory of Atoms in Molecules

(QTAIM) approach as implemented in AIMALL [37].

Results

The replacement of axial H_2O by any of the eight ligands studied causes a shift in the Soret band of NAcCoMP8 to longer wavelengths; the Q bands in the visible region are also red-shifted, but the effect is small. The anionic ligands cause a significantly larger shift than the neutral N-donor ligands studied in this work (Figure 1, Table 1).

Table 1. Changes in the UV-vis spectrum on replacement of H_2O in NAcCoMP8 by a number of neutral and anionic ligands

Ligand	Soret /nm	Q bands /nm	Isosbestic points /nm
H_2O	415	530, 560	
CN^-	424	538, 568	373; 420; 500; 532; 551; 596
N_3^-	416	533, 564	360; 421; 470; 530; 547; 574
NO_2^-	420	532, 565	418; 440; 530; 543; 566
HSO_3^-	423	538, 567	420; 530; 552; 574
py	419	535, 563	418
NMI	420	535, 565	367; 418; 548; 567
MOA	417	532, 563	417
HA	418	533, 563	416; 430; 550

The position of the Soret band of the complexes with these ligands parallels the donor power of the ligand ($H_2O < N_3^- <$ aliphatic N (MOA, HA) < aromatic N (Py, NMI) = $NO_2^- < HSO_3^- < CN^-$) and is very similar to the position of the γ bands of the corresponding cobalamin complexes (Figure S1 of the Supplementary Information). Since the γ band of the corrins [38, 39] and the Soret band of the porphyrins [40] consist of multiple transitions involving principally the near-frontier orbitals of the delocalized π electron system of the macrocycles, these results show that the influence of the axial ligand on the electronic structure of the macrocycle (a *cis* influence) is closely paralleled in the two macrocyclic systems.

The substitution of coordinated H_2O by cyanide proceeds with well-defined isosbestic points (Figure 2). At higher cyanide concentrations a second reaction occurs which is attributed to displacement of the His ligand by cyanide to form a dicyano complex. A fit to the data at low [CN^-] (< 0.04 M) to eqn. 3, and corrected for the acid dissociation constant of HCN and aqua-NAcCoMP8 (eqn .1) gave log $K = 6.04 \pm 0.05$. A

Hill plot of log $[(A_0–A)/(A–A_1)]$ against log $[CN^-]$ gave a slope of 1.03 ± 0.04, confirming the binding of 1 ligand (Figure 3, insert). Similar fits to the data for the second process (Figure 2B) gave log K = 3.50 ± 0.03 and the binding of 0.98 ± 0.04 ligands.

The reaction was studied as a function of temperature and values of ΔH and ΔS were obtained from a plot of ln K against T^{-1} (Figure S2 of the Supplementary Information is an example). Within the concentration range studied with the neutral ligands, only a single process, the substitution of coordinated H_2O, was observed. (At higher ligand concentrations, the substitution of the proximal N-donor ligand, His or dmbzm, is anticipated.) Figures S3 and S4 of the Supplementary Information give examples of the spectroscopic changes observed, and the fits of eqn. 2 to the data, respectively, for NMI.

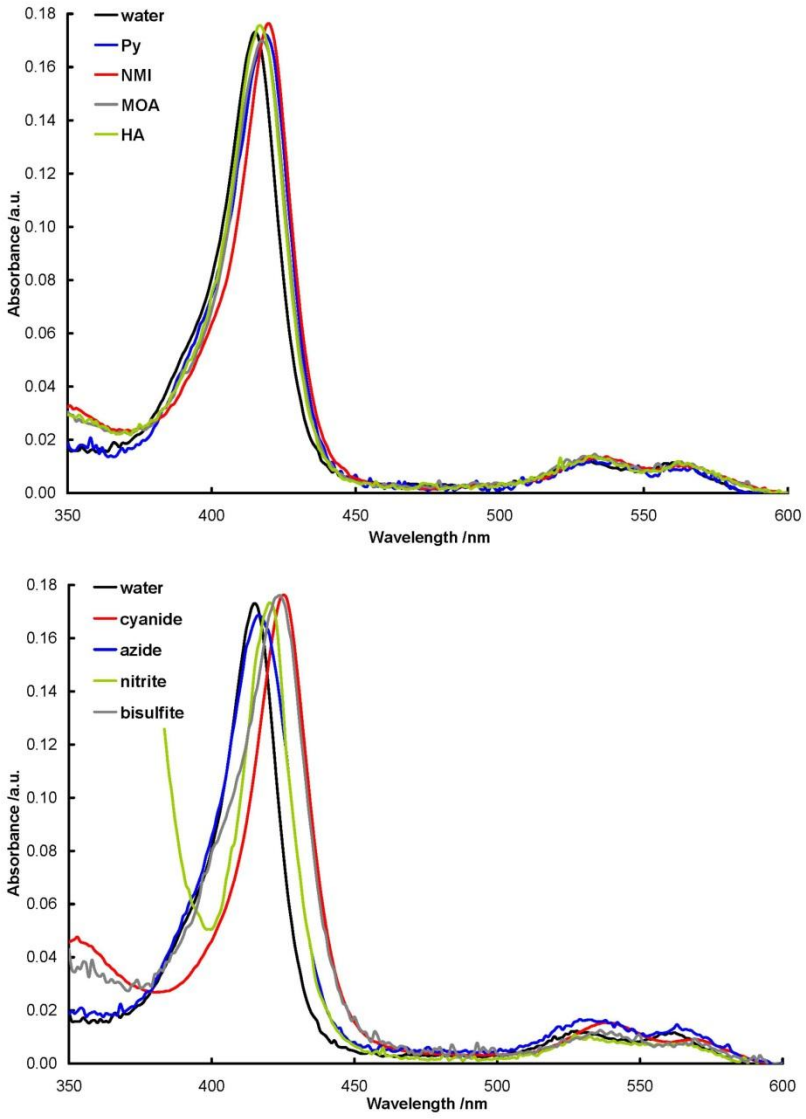

Figure 1. Spectroscopic changes accompanying the replacement of coordinated H_2O by (top) neutral N-donor and (bottom) anionic ligands in NAcCoMP8 (1.1 μM, 0.1 M MOPS buffer, pH 6.8, 25 ^oC (details in Table 1).

The ligand substitution of coordinated H_2O in H_2OCbl^+ proceeded in all cases with well-defined isosbestic points; Figures S5 and S6 of the Supplementary show examples of the data obtained for the reaction of H_2OCbl^+ with NMI.

The values of log *K*, ΔH and ΔS for the ligand substitution reactions of NAcCoMP8 and H_2OCbl^+ are listed in Table 2. Table 3 lists the log *K* values at 25 ^oC as obtained from the van't Hoff plot for H_2OCbl^+ and NAcCoMP8, as well as for various ferric and ferrous microperoxidases.

Examples of fits of the absorbance changes as a function of time that occur on substitution of coordinated H_2O in NAcCoMP8 and in H_2OCbl^+ to a standard exponential equation appropriate for a pseudo first order process are shown in Figure S7 of the Supplementary Information. Figure S8 shows examples of plots of the pH-corrected pseudo first order rate constants, k_I, against ligand concentration. The plots for the reaction of CN^- with NAcCoMP8 pass very close to the origin, whereas those for the reaction of NMI with both NAcCoMP8 and H_2OCbl^+ do not, i.e., the reverse rate constant, k_r, for dissociation of the ligand from the metal is not negligible. Figure S9 gives the Eyring plots obtained for these reactions. Figure S10 shows the Eyring plots for the reverse rate constant for the reaction of NMI with H_2OCbl^+ and with NAcCoMP8. The kinetics data are listed in Table 4.

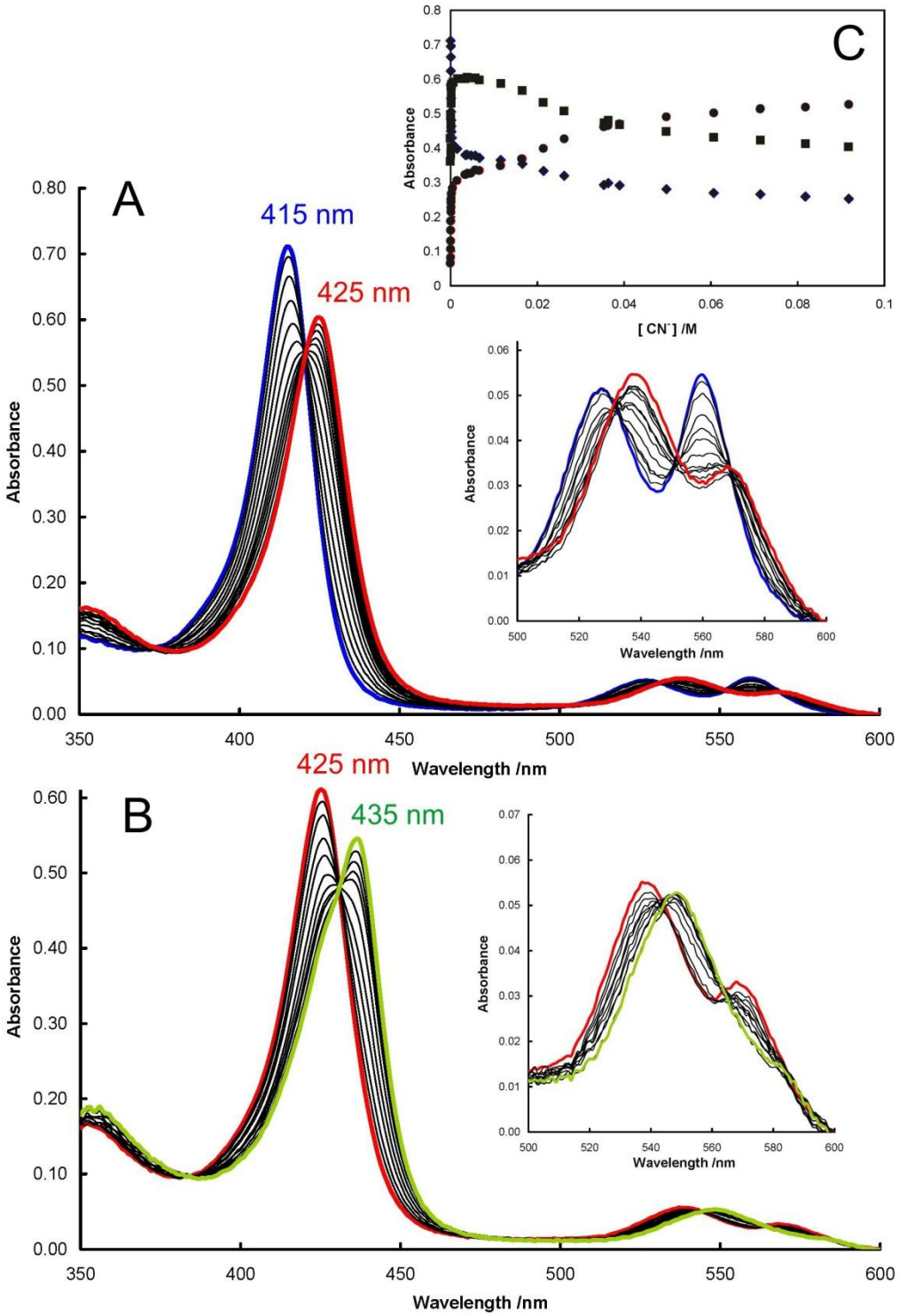

Figure 2. Addition of CN^- to a 4.4 μM solution of NAcCoMP8 (pH 6.95, 25 ^oC) shows two processes each corresponding to the uptake of one ligand (see insert C, shown at 415 nm (diamonds), 425 nm (squares) and 435 nm (circles)). In the first process, A, addition of one CN^- ligand causes the Soret to move from 415 (blue) to 425 nm (red), and the Q bands to move from 527 and 559 nm to 538 and 568 nm, with well-defined isosbestic points This process is complete when $[CN^-] < 40$ mM. The second process, B, occurs at much higher concentrations of CN^- with a further shift in the Soret to 435 nm (green) and the Q bands to 548 and 580 (sh) nm.

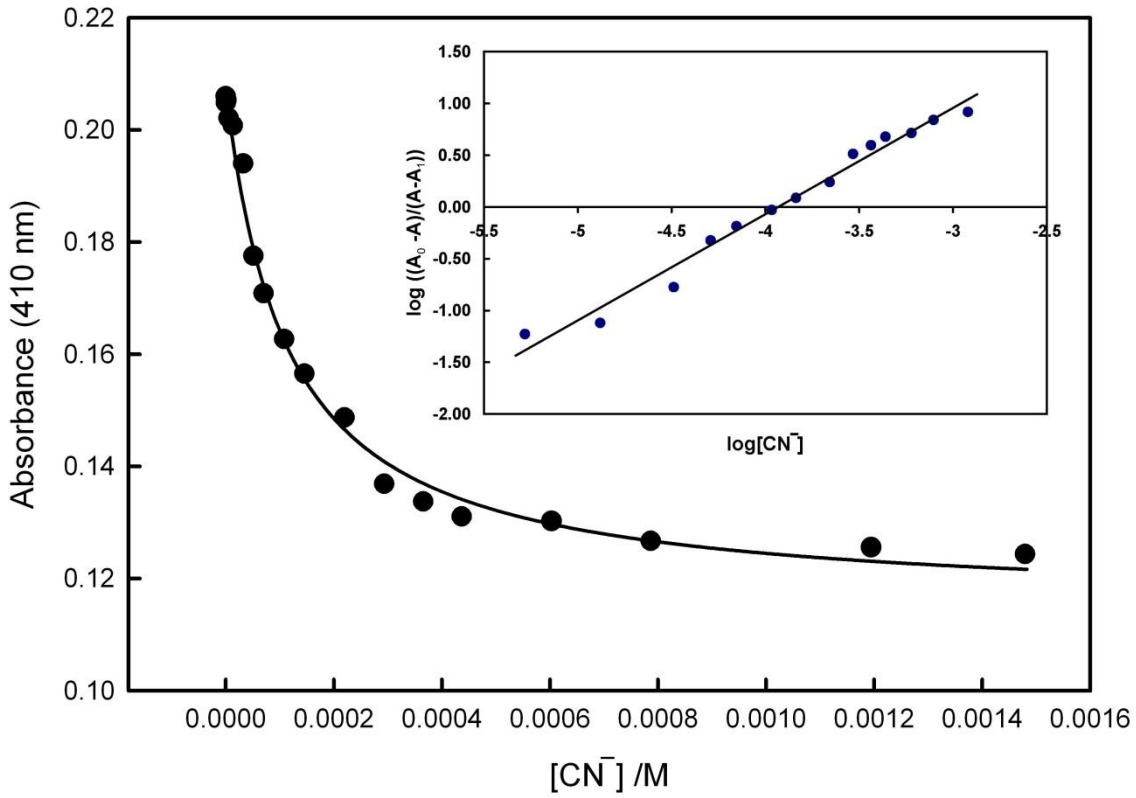

Figure 3. A fit of eqn. 3 to the absorbance change observed on addition of cyanide to 1.6 μM solution of NAcMP8 (pH 6.9, 25 ^{o}C, 0.1 M MOPS buffer). The absorbance at 410 nm is shown as an example. Fits to forty three wavelengths on either side of the isosbestic point gave a weighted log *K* values of 6.04 ± 0.05 after correction for pH (eqn. 1). The insert with slope 1.03 ± 0.04 confirms the binding of one ligand.

Table 2. Equilibrium Constants for the Substitution of Coordinated H_2O in NAcCoMP8 and Aquacobalamin by Some Anionic and Neutral Ligands

Ligand	T /°C	H_2OCbl^+			T /°C	NAcCoMP8		
		log K	ΔH /kJ mol^{-1}	ΔS /J K^{-1} mol^{-1}		log K	ΔH /kJ mol^{-1}	ΔS /J K^{-1} mol^{-1}
CN^-	15.0				5.6	6.64(4)	-47(2)	-42(6)
	20.0				15.4	6.30(5)		
	25.0	≥12[†]			18.0	6.26(6)		
	30.0				20.0	6.15(7)		
	35.0				25.0	6.04(5)		
	40.0				28.0	6.0(1)		
					35.0	5.7(1)		
					45.0	5.6(1)		
HSO_3^-	15.0	5.3(1)	156(9)	644(31)	20.0	3.6(2)	22(2)	143(7)
	20.0	5.8(1)			25.0	3.7(1)		
	25.0	6.5(3)			30.0	3.75(9)		
	30.0	6.9(4)			35.0	3.8(1)		
	35.0	7.1(4)			40.0	3.84(8)		
	40.0	7.5(5)						
N_3^-	15.0	5.23(4)	-29(1)	-1(3)	15.0	2.39(3)	-20(1)	-23(5)
	20.0	5.13(3)			20.0	2.32(6)		
	25.0	5.02(5)			25.0	2.28(6)		
	35.0	4.88(3)			30.0	2.24(7)		
	40.0	4.80(2)			35.0	2.14(5)		
					40.0	2.1(1)		
NO_2^-	15.0	6.2(3)	-47(3)	-44(9)	5.0	3.18(7)	-20(2)	-12(8)
	20.0	6.0(2)			10.0	3.13(9)		
	25.0	5.9(1)			15.0	3.07(6)		
	30.0	5.73(9)			25.0	3.00(4)		
	35.0	5.63(7)			35.0	2.80(6)		
	40.0	5.49(5)			40.0	2.75(8)		
HA	5.5	3.75(6)	100(9)	428(30)	12.0	6.3(6)	-105(13)	-248(44)
	10.0	3.72(6)			15.0	6.3(6)		
	15.0	4.10(6)			18.0	6.1(5)		
	20.0	4.54(6)			20.0	5.7(3)		
	25.0	4.72(4)			25.0	5.5(2)		

Ligand	T /°C	H_2OCbl^+			T /°C	NAcCoMP8		
		log K	ΔH /kJ mol^{-1}	ΔS /J K^{-1} mol^{-1}		log K	ΔH /kJ mol^{-1}	ΔS /J K^{-1} mol^{-1}
	30.0	5.2(2)			30.0	5.4(2)		
	35.0	5.6(1)			35.0	4.6(2)		
	40.0	5.6(2)			40.0	4.7(1)		
MOA	15.0	6.4(3)	-81(7)	-161(23)	10.2	4.48(5)	-64(6)	-138(20)
	20.0	5.9(1)			15.0	4.46(9)		
	25.0	5.78(7)			19.5	4.05(7)		
	30.0	5.6(1)			24.5	3.81(9)		
	35.0	5.22(4)			29.5	3.74(8)		
	40.0	5.11(4)			34.5	3.59(7)		
					39.5	3.5(1)		
Py	15.0	0.98(4)	6.2(0.5)	40(2)	15.0	5.20(6)	-30(3)	-6(9)
	20.0	1.00(4)			20.0	5.07(5)		
	25.0	1.01(3)			25.0	4.93(5)		
	30.0	1.04(2)			30.0	4.87(4)		
	35.0	1.05(2)			35.0	4.82(3)		
	40.0	1.07(5)			40.0	4.74(4)		
NMI	15.0	4.9(1)	-62(3)	-122(11)	10.0	5.26(7)	42(3)	250(11)
	20.0	4.6(1)			15.0	5.49(9)		
	25.0	4.43(7)			25.0	5.76(8)		
	30.0	4.23(4)			35.0	5.93(4)		
	35.0	4.08(4)			40.0	6.03(7)		
	40.0	3.95(5)						

†Ref. [41]. In 80:20 MeOH:H_2O, log K = 12.3(5) [42].

Table 3. Equilibrium Constants at 25 °C for the Substitution of Coordinated H_2O in Aquacobalamin, NAcCoMP8 and Ferric and Ferrous Microperoxidases

Ligand	H_2OCbl^+	Ref	NAcCoMP8	Ref	NAcFe(III)MP8 or NAcFe(III)MP11	Ref
	log *K*		log *K*		log *K*	
CN^-	>12	[41]	6.04	This work	6.76[a]	[11]
					6.55[b]	[13]
HSO_3^-	6.29	This work	3.61	This work		
N_3^-	5.03	This work	2.30	This work	1.4[a]	[43]
					1.33[b]	[13]
					1.45[d]	[44]
NO_2^-	5.94	This work	2.88	This work		
F^-			very low[e]	This work	-0.02[c]	[45]
					0.08[b]	[13]
SCN^-	3.10		very low[e]	This work	-0.16[a]	[43]
					-0.52[d]	[44]
					-0.17[b]	[13]
HA	4.83	This work	5.45	This work	2.9[a]	[11]
MOA	5.79	This work	4.01	This work	2.14[a]	[11]
Py	1.00	This work	4.94	This work	2.62[a]	[11]
					2.49[f]	[46]
					2.65[d]	[47]
NMI	4.49	This work	5.70	This work	4.17[a]	[11]
Im					4.076[a]	[11]
					4.16[b]	[13]
					4.34[g]	[48]
					4.45[d]	[49]
					4.05[h]	[50]

[a]NAcFe(III)MP8. [b]NAcFe(III)MP11. [c]Fe(III)MP8 in 50% ethylene glycol. [d]Fe(III)MP8 in 20% MeOH. [e]The low value of *K* required a high concentration of the ligand; the high ionic strength caused aggregation of NAcCoMP8 and precluded the determination of *K*. [f]Fe(III)MP11. [g]Fe(III)MP9 in 20% MeOH. [h]Fe(III)MP6

Table 4. Rate Constants and Activation Parameters for the Reaction of Cyanide and N-Methylimidazole with NAcCoMP8 and Aquacobalamin

Reaction	**Temp** /^{o}C	k_{II} /M^{-1} s^{-1}	$\Delta H^{‡}$ kJ mol^{-1}	$\Delta S^{‡}$ J K^{-1} mol^{-1}	k_{II} (25 ^{o}C) /M^{-1} s^{-1}	k_r * /s^{-1}	$\Delta H^{‡}$ kJ mol^{-1}	$\Delta S^{‡}$ J K^{-1} mol^{-1}	k_r (25 ^{o}C) /s^{-1}
		(× 10^{2})							
CN^{-} + NAcCoMP8	15.1	0.36(2)	75(3)	46(9)	112				
	20.3	0.61(2)							
	25.0	1.10(4)							
	30.0	1.82(5)							
	35.2	2.8(2)							
CN^{-} + H_2OCbl^{+} †			51.9(1.3)	-25.3(3.8)	237				
NMI + NAcCoMP8		(× 10^{2})				(× 10^{-4})			
	10.7	3.1(9)	66(5)	34(16)	1.0×10^{3}	6(41)	86(25)	-5(99)	3.3×10^{-3}
	13.2	4.5(9)				4(6)			
	15.1	5.6(2.0)				19(7)			
	20.1	7.8(5)				8(16)			
	24.5	13.3(5)				29(7)			
	30.5	2.2(1.3)				82(32)			
						(× 10^{-4})			
NMI + B12a	10.4	2.6(1)	73(3)	21(11)	12		146(26)	196(83)	1.2×10^{-2}
	11.0	2.82(9)							
	15.0	6.6(7)							
	20.0	8.72(3)				19(3)			
	25.0	16(2)				7(9)			
	30.0	20(2)				147(32)			
	34.7	37(1)				152(7)			
	39.3	52(3)				443(15)			

*Rate constant for the reverse reaction. †Data from Ref. [14].

4. Discussion

4.1 Log K values. The equilibrium constants at 25 °C for substitution of coordinated H_2O in NAcCoMP8 and in H_2OCbl^+ are compared in Figure 4. The log *K* for coordination of Py by H_2OCbl^+ is anomalously low. There are no crystal structures of a pyridine complex of a cobalt corrinoid. Entries in the Cambridge Structural Database [51] show that Py complexes of cobaloximes, in which the *trans* ligand is also Py, have axial Co–N bond lengths of 1.99(3) Å (Table S1 of the Supplementary Information). In porphyrins, the Co–N bond length to Py *trans* to an N-donor ligand is 2.01(4) Å. In Co(III) corroles, Py *trans* to Py has an average bond length of 1.99(2) Å. In three Py complexes of Co(III) in which the *trans* ligand is NH_3 and the equatorial ligands are either NH_3 or ethylenediamine, the Co–N bond length to Py is 1.967(8) Å. Thus, in the relatively sterically undemanding environments of simple pentammine complexes, porphyrins, cobaloximes and corroles, the Co–N bond to Py is very similar, on average 1.99(2) Å, and Co(III) behaves in a very similar fashion towards Py in a wide range of complexes. The upper, or *β* coordination site of a cobalamin is very sterically crowded [52, 53] with C26, C37, C46 and C54 adopting sentinel-like positions impeding an approach to the metal (Figure S11 of the Supplementary Information). We therefore presumed that the low log *K* value for coordination of Py is a consequence of the steric demands of the corrin macrocycle.

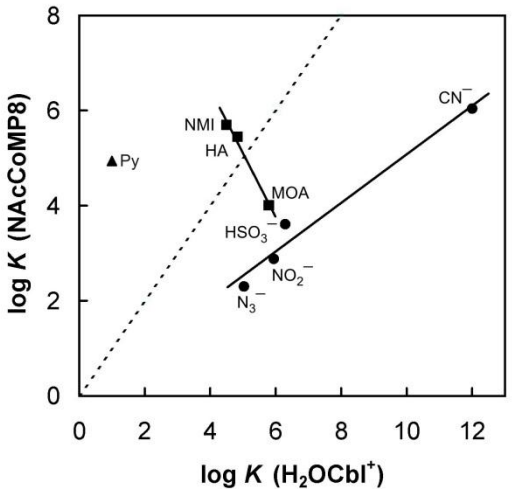

Figure 4. A comparison of log *K* values (25 °C) for substitution of coordinated H_2O in H_2OCbl^+ and in NAcCoMP8. The dotted line is the equi-value line.

To verify this, we performed DFT calculations on a truncated version of a cobalamin (see Experimental) with Py, imidazole and NO_2^- as axial ligands, the latter two to verify the performance of the computational method chosen against the available crystal structures of $ImCbl^+$ and $HisCbl^+$ [30] and NO_2Cbl [4, 54]. We also measured the corrin fold angle of the complexes (the angle between the mean planes through N21, C4, C5, C6, N22, C9 and C10, and N24, C16, C15, C14, N23, C11 and C10, respectively) as the steric demands of the *β* are expected to flatten the corrin ring [52]. Our model of $ImCbl^+$ had a Co–N bond length to

imidazole of 1.996 Å (cf. 1.939 and 1.951 Å in the crystal structures of imidazole- and $HisCbl^+$, respectively); the corrin fold angle was 9.2° (11.8 and 11.9° in the crystal structures). The Co–N bond length to NO_2^- in our model of the nitrite complex was 1.957 Å with a corrin fold angle of 19.8° (cf. 1.939 Å and 14.5° [4, 54]; and 1.942 Å, 17.7° and 1.912 Å, 17.8° [4, 54] in the crystal structures). Thus, our DFT calculations somewhat overestimate the bond lengths to the *β* ligand but satisfactorily reproduce the corrin fold angles. In particular, it is noteworthy that the much smaller NO_2^- ligand allows for a significantly more folded corrin than the sterically more demanding imidazole ligand.

The Co–N bond to Py in the $PyCbl^+$ model was found to be 2.045 Å and the corrin fold angle was 6.8°, confirming the steric demands of Py as a ligand, and rationalizing the observed low log *K* value. An examination of the geometry-optimized structure (Figure S12) shows that the Py is constrained to the C5—C15 vector of the corrin by the sentinel C26, C37, C47 and C54 substituents of the corrin. The H atoms on the carbons *α* to the Py N atom come into van der Waals contact with C5 and C15. This explains the relatively long $Co–N_{Py}$ bond and small corrin fold angle.

The other rigid planar ligand studied, NMI, is expected to be much less sterically demanding as the C–N–C angle of 105(3)° (460 observations in the CSD in 304 compounds where an imidazole is not coordinated to a metal ion) is significantly smaller than the equivalent angle in Py (117(3)°, *n* = 1306 in 775 compounds) so that the H atoms on the *α* carbons should have less contact with the macrocycle. Indeed, there are two structures of a cobalamin in which the *β* ligand is imidazole or a derivative: $ImCbl^+$ itself ($Co–N_{Im}$ = 1.939 Å) [30] and $HisCbl^+$ ($Co–N_{His}$ = 1.951 Å) [30]. The average $Co–N_{Im}$ bond length in bis-imidazole Co(III) porphyrins is very similar, 1.95(2) Å, with the shortest bond reported at 1.905 Å and the longest as 1.972 Å [55-57]. Our model of $ImCbl^+$ (Figure S13) shows that imidazole, like Py (Figure S12) is constrained by the sentinel substituents of the corrin. Although its *α* hydrogen atoms still come into van der Waals contact with C5 and C15, they are further away than in Py (data in Figures S12 and S13).

A striking feature of Figure 4 is that all anionic ligands bind more strongly to H_2OCbl^+ than to NAcCoMP8, and the log *K* values in the two systems parallel each other. Neutral ligands, on the other hand, tend to bind more strongly to NAcCoMP8 than to H_2OCbl^+ (although MOA is an exception) and there appears to be an inverse relationship

between the log *K* values in the two systems (this must be a tentative conclusion, as it is based on only three observations; a further exploration of this is planned and will be reported elsewhere).

Other than the very different steric demands of a porphyrin, with its near-planar macrocycle, and the corrin, with its sentinel peripheral substituents discussed above, a significant difference between the two systems is that the corrin macrocycle is a mono-anion; in Co(III) corrinoids the net charge at the metal center is +2 (assuming that in the cobalamins the charge on the phosphate, some 9 Å away, is too remote to influence matters). By contrast a porphyrin is a di-anion and the net charge at the metal center in Co(III) porphyrins is therefore +1 (again assuming that the remote charges, in this case on the propionate side chains between about 5.5 and 8.5 Å away depending on the side chain orientation, do not influence matters). This therefore suggests that a columbic attraction between the charge at the metal center and an axial anionic ligand influences the value of log *K*, and anions will bind more strongly to cobalamin than to a Co(III) porphyrin.

By determining log *K* as a function of temperature, and hence being able to calculate ΔH and ΔS values for these ligand substitution reactions, we hoped to gain further insight into the factors that control the magnitude of log *K* and establish whether enthalpic or entropic effects were primarily responsible for discrimination between the two systems. We find that there is a strong compensation effect between the two parameters in both systems (Figure S14) such that negative values of ΔH tend to be offset by positive values of ΔS, and vice-versa. This compensation effect causes a leveling out of log *K* values. Omitting Py (because steric effects probably dominate, see above) and CN^- (log *K* for its reaction with H_2OCbl^+ is too large for a reliable determination of *K* let alone ΔH and ΔS — for example, estimates of log *K* vary from >12 [41], to 12.3(5) in 80:20 MeOH:H_2O [42], to 14.1 [58]) we find that ΔH values (and hence ΔS values, because of their correlation, Figure S14) for the anionic ligands vary in a similar fashion ($HSO_3^- > N_3^- > NO_2^-$) in the two systems. This is not the case for the neutral ligands (HA > NMI > MOA for H_2OCbl^+ but NMI > MOA > HA for NAcCoMP8). For this reason, log *K* values parallel each other in the two systems when binding anions, but appear to be inversely correlated for the binding of the neutral ligands (Figure 4).

The order of log *K* for coordination the anions to both H_2OCbl^+ and to NAcCoMP8 (Table 3) approximately parallels the pK_a [59] of their conjugate acid (HCN, 9.04; H_2SO_3, 6.85; HN_3, 4.44; HNO_2, 2.94; HF, 2.95; HSCN, –0.9) — although on this basis one would expect log *K* for NO_2^- < log *K* for N_3^- and for F^- to have a reasonably high log *K* value. Nevertheless, this suggests that the affinity of an anion for Co(III) in both H_2OCbl^+ and NAcCoMP8 is similar to its affinity for the proton. However, the two systems behave differently towards the neutral ligands. For H_2OCbl^+, log *K* values correlate inversely with the pK_a of the ligand (the pK_a values vary as NMI, 7.10 > HA, 5.96 > MOA, 4.60, while log *K* varies as MOA (5.97) > HA (4.83) > NMI (4.49)). For NAcCoMP8 there is a direct correlation (log *K* for NMI (5.70) > HA (5.45) > MOA (4.01)).

4.2 DFT modeling – Structure. To gain insight into the differences between the corrin and the porphyrin systems, we performed DFT calculations on simple models of the two systems with imidazole as the lower axial ligand, and our range of neutral and anionic ligands as the upper ligand. To compensate for the anomalous result with Py, we included NH_3 in the calculations although we were unable to obtain reliable values for log *K* with NAcMP8 because of aggregation due to the inevitably high ionic strength that arises from using NH_4Cl as the source of the ligand.

Table 5 gives the bond lengths to the axial ligands in the modeled structures. In all cases we find that the bond lengths in the corrin system are longer than in the porphyrin, as expected given the sterically more crowded environment of the metal in the former. Exact parallels are difficult to find in the crystal structure literature; nevertheless, the Co–N_{im} bond length in $[Co(TPP)(NMI)_2]^+$ (1.941 and 1.943 Å) [56] and in $[Co(TPP)(Im)_2]^{2+}$ (1.905 and 1.945 Å, respectively, in the two molecules in the unit cell) [57] is indeed somewhat shorter than in the B_{12} analog in which the dmbzm base of B_{12} is replaced by imidazole (1.968 Å) [60]. The average difference of the Co–L bond length between the corrin system and the porphyrin system ($\Delta r_{\text{Corrin–Porphyrin}}$, Table 5) for the neutral ligands, 0.025(3) Å, is larger than for the anions (0.015(10) Å). We attribute this to the increased coulombic interaction between the anionic ligands and the greater charge on the metal center in the corrin system; in other words, whilst the bonds to the axial anionic ligands remain longer in corrin than in porphyrin, they are shorter than might have been expected based on the results obtained with the neutral ligands.

Table 5. Bond lengths of the axial bonds in modeled (M06L/SVP/SVPFit) corrin and porphyrin structures (L–CoN_4–Im), N_4 = porphyrin or corrin

	Corrin		**Porphyrin**			
	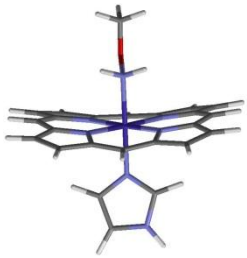		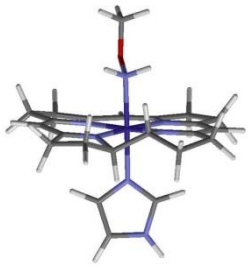			
L					**$\Delta r_{Corrin–Porphyrin}$**	
	Co–L /Å	**Co–Im /Å**	**Co–L /Å**	**Co–Im /Å**	**Co–L /Å**	**Co–Im /Å**
NH_3	2.024	1.969	1.996	1.952	0.028	0.017
NH_2OH	2.027	1.966	2.000	1.949	0.027	0.017
NH_2OMe	2.021	1.968	1.996	1.950	0.025	0.018
Im	1.988	1.988	1.967	1.968	0.021	0.020
CN^-	1.874	2.077	1.871	2.071	0.003	0.006
NO_2^-	1.969	2.078	1.943	2.075	0.026	0.003
HSO_3^-	2.260	2.054	2.245	2.054	0.013	0.000
N_3^-	1.968	2.034	1.950	2.026	0.018	0.008

4.3 DFT modeling – QTAIM analysis. We have already demonstrated the usefulness of QTAIM for characterizing the bonding in the complexes of the first transition series [61-66]. We therefore performed a QTAIM analysis on the wavefunction describing the electron density in the energy-minimized model structures referred to in 4.2, focusing attention on the bonds to the axial ligands. The results are given in Table S3 of the Supplementary Information.

The electron density, ρ, at a bond critical point (bcp) is a measure of the strength of the chemical bond [67-74]. Since the bond lengths between Co(III) and the axial bonds are longer in the corrin than in the porphyrin, their ρ values are lower (Table S3). There is a good correlation between the bond lengths and the ρ values (Figure S15A) but no significant correlation between ρ and either log K values or ΔH for coordination of the ligands by the Co(III) complexes (Figure S15B,C); this suggests that, while the strength of the bond

between the metal and the axial ligand will undoubtedly affect the value of log K and ΔH, other factors are clearly important.

A QTAIM analysis also provides insight into the nature of the bonding between the metal and the axial ligand. Briefly, for a covalent interaction, ρ is usually > 0.1 au [75] and the Laplacian of electron density, $\nabla^2\rho$, which may be positive or negative [75] (but usually negative [76]), is usually of the same order as ρ. The ratio of the potential and kinetic energy densities at the bcp, $|V|/G > 2$ [77]. In the case of an ionic interaction ρ is close to zero [75]), $\nabla^2\rho$ is positive, and $|V|/G < 1$. When $1 < |V|/G < 2$, the bonding is of intermediate character. In the case of metal-ligand bonding, the total energy density $H = V + G$ is usually negative and close to zero (as found for ionic interactions) but $\nabla^2\rho > 0$, as found for covalent interactions [78]. An examination of the results given in Table S3 show clearly that the bonds between Co(III) and all axial ligands are predominantly ionic (ρ close to zero, $\nabla^2\rho > 0$, and $|V|/G$ close to 1) with some covalent character present when the axial ligand is an anion, especially in the case of CN^-. The bond between this ligand and the metal is the strongest amongst all the complexes studied (the ρ values are largest) suggesting, at least in part, an explanation of the high log K values for this ligand. There is a correlation between log K and $|V|/G$ for the anionic ligands, but not for the neutral N-donor ligands (Figure S16). In agreement with this, the values of the delocalization index, DI(Co,L), which is a measure of the average number of electrons delocalized or shared between atoms Co and the donor atom of the axial ligand L, are larger for the anionic ligands than for the neutral ligands.

Thus, two conclusions emerge: firstly, electron-rich anionic ligands induce a significant covalency in their bond to Co(III) in both corrins and porphyrins, whereas the bonding between the metal and neutral N-donor ligands is predominantly ionic; secondly, the extent of the covalency appears to be an important factor in determining the stability of the resultant complex. The extent of this covalent character is very similar in the corrin and porphyrin systems; there must therefore be another important factor in determining log K to explain why anionic ligands are bound more tightly by Co(III) in a corrin than in a porphyrin. We suggest this is a coulombic interaction between the ligand and the residual charge at the metal center.

The ellipticity of a bond is defined as $\varepsilon = |\lambda_1|/|\lambda_2| - 1$, where λ_1 and λ_2 are the eigenvalues of the Hessian matrix of the electron density at the bcp along mutually

perpendicular axes which are themselves perpendicular to the bond path; it is a therefore a function of the ratio of the rate of electron density decrease in the two directions perpendicular to the bond path at the bcp [79]. In the case of significant π bonding between two atoms (cf. the N–C and the C–C bond of imidazole, Table S3), $|\lambda_1| > |\lambda_2|$ and ε will be significantly greater than 1.

We note that in the anionic complexes of both systems, the values of $|\lambda_1|$ and $|\lambda_2|$, while still small compared to those of the delocalized N–C and C–C bonds in imidazole, are significantly larger than in Co(III)–L bonds where L is a neutral ligand. Since $|\lambda_1| \approx |\lambda_2|$ when L = CN^-, $\varepsilon \approx 0$); but $|\lambda_1| > |\lambda_2|$ when L = NO_2^-, N_3^- or HSO_3^- and ε is significantly greater than in other complexes. This suggests some multiple bond character between the metal and the ligand (and may thus contribute to the larger values of *DI*(Co,L) noted above). In the case of CN^-, the similar values of λ_1 and λ_2 indicate that both frontier π^* orbitals are involved in the bonding, whilst in the case of NO_2^- it is the single frontier orbital with π symmetry, located on the O atoms of the ligand, that is involved. In the azido complexes, only one of the frontier π^* appears to be involved since $|\lambda_1| > |\lambda_2|$. In the case of HSO_3^-, $|\lambda_1| \approx |\lambda_2|$ suggesting that multiple bonding involving more than one of the O atoms of the ligand may be involved.

4.4 Kinetics. The kinetics data in Table 4 show rate constants and activation parameters for the substitution of H_2O coordinated to Co(III) *trans* to an imidazole derivative by CN^- and NMI. H_2OCbl^+ is significantly more labile towards substitution by CN^- than NAcCoMP8; using the activation parameters determined, we find that the second rate constant is more than twice as large at 25 ^oC (240 M^{-1} s^{-1}) for the former than for the latter (103 M^{-1} s^{-1}). The difference arises from a much smaller $\Delta H^‡$ value for the reaction with H_2OCbl^+, which is somewhat, but not completely, compensated for by a much more negative $\Delta S^‡$. If the latter value were the same in both systems, then k_{II} would be 10^4 larger for the reaction with H_2OCbl^+ than for that with NAcCoMP8. As we pointed out in our recent study comparing the kinetics of ligand substitution on a aquacyanocobester and a cobester in which the conjugation of the corrin is interrupted at the C5 position [80], this compensation effect masks the very significant effect of the change in the electronic properties of the equatorial ligand on the rate of substitution of the axial ligand, reflected, as we argued [80] in the very different values of $\Delta H^‡$.

The intimate mechanism of the ligand substitution reactions of H_2OCbl^+ is best described as an interchange mechanism under dissociative activation, I_d [14, 24-26] – see Introduction; it is likely to be very similar on a Co(III) porphyrin [81-83]. Thus, the transition state of the rate determining step will feature significant bond breaking between Co(III) and departing H_2O, and some extent of bond formation between the metal and the entering ligand. That $\Delta H^{\ddagger}$ for the reaction of H_2OCbl^+ with CN^- is less positive than for its reaction with NAcCoMP8, while conversely $\Delta S^{\ddagger}$ is more negative, is consistent with a transition state that occurs earlier along the reaction coordinate and in which there is greater participation of incoming CN^- in that transition state. This is also consistent with our observation that log *K* for coordination of anionic CN^- by H_2OCbl^+ is larger than log *K* for its coordination by NAcCoMP8.

By contrast, the reaction of NMI occurs faster with NAcCoMP8 than with H_2OCbl^+ due to a smaller $\Delta H^{\ddagger}$ and a somewhat larger value of $\Delta S^{\ddagger}$. This again parallels the log *K* values; we interpret this by envisaging that the greater thermodynamic stability of the NMI complex with the cobalt porphyrin compared to its complex with the cobalt corrin causes a greater involvement of the entering ligand in the transition state. We therefore conclude that there is a correlation between the thermodynamic stability of Co(III) complexes of corrin and porphyrins and the rate of substitution of axially coordinated H_2O to form these complexes.

There is no doubt that Co(III) is more labile in these macrocyclic systems than in acyclic pentammine complexes, for example (see the Introduction to the accompanying paper). But Co(III) is not necessarily more labile in a corrin than in a porphyrin; the nature of the incoming ligand will determine which of these two macrocyclic systems is the more labile. A more complete investigation involving a wider range of both anionic and neutral ligands is planned and will be reported elsewhere.

Acknowledgment. This work was funded by grants from the Department of Science and Technology's South African Research Chairs Initiative, administered by the National Research Foundation (Pretoria), and the University of the Witwatersrand.

References

[1] S. Mathura, D. Sannasy, A.S. De Sousa, H.M. Marques, J. Inorg. Biochem., Submitted.
[2] H.M. Marques, J.H. Marsh, J.R. Mellor, O.Q. Munro, Inorg. Chim. Acta, vol. 170, 1990, pp. 259-269.
[3] J.M. Pratt, in: R. Banerjee (Ed.), Chemistry and Biochemistry of B_{12}, John Wiley & Sons, Inc., New York, 1999, pp. 73-112.
[4] C.B. Perry, M.A. Fernandes, K.L. Brown, X. Zou, E.J. Valente, H.M. Marques, Eur. J. Inorg. Chem., 2003, pp. 2095-2107.
[5] H.M. Marques, L. Knapton, X. Zou, K.L. Brown, J. Chem. Soc., Dalton Trans., 2002, pp. 3195-3200.
[6] L. Knapton, H.M. Marques, Dalton Trans., 2005, pp. 889-895.
[7] L. Knapton, H.M. Marques, S. Afr. J. Chem., vol. 59, 2006, pp. 43-47.
[8] M. Hamza, J. Chem. Soc., Dalton Trans., 2002, pp. 2831-2836.
[9] D. Zheng, R.L. Birke, J. Am. Chem. Soc., vol. 124, 2002, pp. 9066-9067.
[10] M. Wolak, G. Stochel, M. Hamza, R. Van Eldik, Inorg. Chem., vol. 39, 2000, pp. 2018-2019.
[11] H.M. Marques, O.Q. Munro, T. Munro, M. de Wet, P.R. Vashi, Inorg. Chem., vol. 38, 1999, pp. 2312-2319.
[12] H.M. Marques, I. Cukrowski, P.R. Vashi, J. Chem. Soc., Dalton Trans., 2000, pp. 1335-1342.
[13] C.B. Perry, T. Chick, A. Ntlokwana, G. Davies, H.M. Marques, J. Chem. Soc., Dalton Trans., 2002, pp. 449-457.
[14] W.W. Reenstra, W.P. Jencks, J. Am. Chem. Soc., vol. 101, 1979, pp. 5780-5791.
[15] H.M. Marques, K.L. Brown, D.W. Jacobsen, J. Biol. Chem., vol. 263, 1988, pp. 12378-12383.
[16] H.M. Marques, D.A. Baldwin, J.M. Pratt, J. Inorg. Biochem., vol. 29, 1987, pp. 77-91.
[17] W.C. Randall, R.A. Alberty, Biochemistry, vol. 5, 1966, pp. 3189-3193.
[18] W.C. Randall, R.A. Alberty, Biochemistry, vol. 6, 1967, pp. 1520-1525.
[19] D. Thusius, J. Am. Chem. Soc., vol. 93, 1971, pp. 2629-2635.
[20] D. Thusius, J. Chem. Soc., Chem. Commun., 1968, pp. 1183.
[21] C.K. Poon, Coord. Chem. Rev., vol. 10, 1973, pp. 1-35.
[22] H.M. Marques, J. Chem. Soc., Dalton Trans., 1991, pp. 339-341.
[23] H.M. Marques, J. Chem. Soc., Dalton Trans. , 1991, pp. 1437-1442.
[24] G. Stochel, R. van Eldik, Inorg. Chem., vol. 29, 1990, pp. 2075-2077.
[25] H.M. Marques, J.C. Bradley, L.A. Campbell, J. Chem. Soc., Dalton Trans., 1992, pp. 2019-2027.
[26] H.M. Marques, O.Q. Munro, B.M. Cumming, C. de Nysschen, J. Chem. Soc., Dalton Trans., 1994, pp. 297.
[27] P.R. Vashi, H.M. Marques, J. Inorg. Biochem., vol. 98, 2004, pp. 1471-1482.
[28] H.M. Marques, O.Q. Munro, M.L. Crawcour, Inorg. Chim. Acta, vol. 196, 1992, pp. 221-229.
[29] M.J.T. Frisch, G. W.; Schlegel, H. B.; Scuseria, G. E.; Robb, M. A.; Cheeseman, J. R.; J. A. Montgomery, J.; Vreven, T.; Kudin, K. N.; Burant, J. C.; Millam, J. M.; Iyengar, S. S.; Tomasi, J.; Barone, V.; Mennucci, B.; Cossi, M.; Scalmani, G.; Rega, N.; Petersson, G. A.; Nakatsuji, H.; Hada, M.; Ehara, M.; Toyota, K.; Fukuda, R.; Hasegawa, J.; Ishida, M.; Nakajima, T.; Honda, Y.; Kitao, O.; Nakai, H.; Klene, M.; Li, X.; Knox, J. E.; Hratchian, H. P.; Cross, J. B.; Adamo, C.; Jaramillo, J.; Gomperts, R.; Stratmann, R. E.; Yazyev, O.; Austin, A. J.; Cammi, R.; Pomelli, C.; Ochterski, J. W.; Ayala, P. Y.; Morokuma, K.; Voth, G. A.; Salvador, P.; Dannenberg, J. J.; Zakrzewski, V. G.; Dapprich, S.; Daniels, A. D.; Strain, M. C.; Farkas, O.; Malick, D. K.; Rabuck, A. D.; Raghavachari, K.; Foresman, J. B.; Ortiz, J. V.; Cui, Q.; Baboul, A. G.; Clifford, S.; Cioslowski, J.; Stefanov, B. B.; Liu, G.; Liashenko, A.; Piskorz, P.; Komaromi, I.; Martin, R. L.; Fox, D. J.; Keith, T.; Al-Laham, M. A.; Peng, C. Y.; Nanayakkara, A.; Challacombe, M.; Gill, P. M. W.; Johnson, B.; Chen, W.; Wong, M. W.; Gonzalez, C.; Pople, J. A. , Gaussian 09, Gaussian, Inc.: Wallingford CT, 2009.
[30] L. Hannibal, S.D. Bunge, R. van Eldik, D.W. Jacobsen, C. Kratky, K. Gruber, N.E. Brasch, Inorg. Chem., vol. 46, 2007, pp. 3613-3618.

[31] Y. Zhao, D.G. Truhlar, J. Chem. Phys., vol. 125, 2006, pp. 194101.
[32] A. Schaefer, H. Horn, R. Ahlrichs, J. Chem. Phys., vol. 97, 1992, pp. 2571.
[33] K. Eichkorn, O. Treutler, H. Ohm, M. Ahser, R. Ahlrichs, Chem. Phys. Lett., vol. 240, 1995, pp. 283.
[34] K. Eichkorn, F. Weigend, O. Treutler, R. Ahlrichs, Theor. Chem. Acc., vol. 97, 1997, pp. 119.
[35] B.I. Dunlap, J. Chem. Phys., vol. 78, 1983, pp. 3140-3142.
[36] B.I. Dunlap, J. Mol. Struct. (Theochem), vol. 529, 2000, pp. 37-40.
[37] v. AIMALL, T.A. Keith, TK Gristmill Software, Overland, Park KS, USA (aim.tkgristmill.com), 2011.
[38] M. Gouterman, J. Chem. Phys., vol. 30, 1959, pp. 1139-1161.
[39] I. Navizet, C.B. Perry, P.P. Govender, H.M. Marques, J. Phys Chem. B, vol. in press, 2012.
[40] M.W. Makinen, A.K. Churg, in: A.B.P. Lever, H.B. Gray (Eds.), Iron Porphyrins, Part 1, Addison-Wesley, Reading, MA, 1983, pp. 141-235.
[41] G.C. Hayward, H.A.O. Hill, J.M. Pratt, N.J. Vanston, R.J.P. Williams, J. Chem. Soc. A, 1965, pp. 6485-6493.
[42] C.F. Zipp, S. Mathura, J.P. Michael, M.A. Fernandes, H.M. Marques, unpublished results.
[43] H.M. Marques, I. Cukrowski, P.R. Vashi, J. Chem. Soc., Dalton Trans., 2000, pp. 1335-1342.
[44] H.M. Marques, University of the Witwatersrand, Johannesburg, 1986.
[45] Y.P. Huang, R.J. Kassner, J. Biol. Chem., vol. 256, 1981, pp. 5327-5331.
[46] H.A. Harbury, P.A. Loach, J. Biol. Chem., vol. 235, 1960, pp. 3646-3653.
[47] M.S.A. Hamza, J.M. Pratt, J. Chem. Soc., Dalton Trans., 1993, pp. 1647-1650.
[48] D.A. Baldwin, M.B. Mabuya, H.M. Marques, S. Afr. J. Chem., vol. 40, 1987, pp. 103-110.
[49] D.A. Baldwin, H.M. Marques, J.M. Pratt, J. Inorg. Biochem., vol. 27, 1986, pp. 245-254.
[50] M.M.M. Saleem, M.T. Wilson, Inorg. Chim. Acta, vol. 153, 1988, pp. 99-104.
[51] CCDC, Cambridge, UK, 2011.
[52] J.P. Glusker, in: D. Dolphin (Ed.), B_{12}, vol. 1, Wiley-Interscience, New York, 1982, pp. 23-107.
[53] K.L. Brown, X. Zou, H.M. Marques, J. Mol. Struct. (Theochem), vol. 453, 1998, pp. 209-224.
[54] G. Garau, S. Geremia, L.G. Marzilli, G. Nardin, L. Randaccio, G. Tauzher, Acta Cryst., Sec. B, 2003, pp. 51-59.
[55] J. Li, B.C. Noll, A.G. Oliver, G. Ferraudi, A.G. Lappin, W.R. Scheidt, Inorg. Chem., vol. 49, 2010, pp. 2398.
[56] H. Bang, J.O. Edwards, J. Kim, R.G. Lawler, K. Reynolds, W.J. Ryan, D.A. Sweigart, J. Am. Chem. Soc., vol. 114, 1992, pp. 2843.
[57] J.W. Lauher, J.A. Ibers, J. Am. Chem. Soc., vol. 96, 1974, pp. 4447.
[58] N.R. de Tacconi, D. Lexa, J.M. Saveant, J. Am. Chem. Soc., vol. 101, 1979, pp. 467.
[59] A.E. Martell, R.M. Smith, R.J. Motekaites, NIST, Gaithersburg, MD, 2004.
[60] B. Kräutler, R. Konrat, E. Stupperich, G. Färber, K. Gruber, C. Kratky, Inorg. Chem., vol. 33, 1994, pp. 4128-4139.
[61] P.R. Varadwaj, I. Cukrowski, H.M. Marques, J. Phys. Chem. A, vol. 112, 2008, pp. 10657-10666.
[62] P.R. Varadwaj, H.M. Marques, Phys. Chem. Chem. Phys., vol. 12, 2010, pp. 2126-2138.
[63] P.R. Varadwaj, H.M. Marques, Theor. Chem. Acc., vol. 127, 2010, pp. 711-725.
[64] P.R. Varadwaj, A. Varadwaj, H.M. Marques, J. Phys. Chem. A, vol. 115, 2011, pp. 5592-5601.
[65] P.R. Varadwaj, A. Varadwaj, G.H. Peslherbe, H.M. Marques, J. Phys. Chem. A, vol. 115, 2011, pp. 13180-13190.
[66] P.R. Varadwaj, I. Cukrowski, C.B. Perry, H.M. Marques, J. Phys. Chem. A, vol. 115, 2011, pp. 6629-6640.
[67] S.T. Howard, T.M. Krygowski, Can. J. Chem., vol. 75, 1997, pp. 1174-1181.
[68] S.E. O'Brien, P.L. Popelier, Can. J. Chem., vol. 77, 1999, pp. 28-36.
[69] R.F.W. Bader, C.F. Matta, J. Phys. Chem. A vol. 108 2004, pp. 8385-8394.

[70] I. Vidal, S. Melchor, I. Alkorta, J. Elguero, M.R. Sundberg, J.A. Dobado, Organometallics, vol. 25, 2006, pp. 5638-5647.
[71] L. González, O. Mó, M. Yáñez, J. Elguero, J. Mol. Str., vol. 371, 1996, pp. 1-10.
[72] E. Espinosa, M. Souhassou, H. Lachekar, C. Lecomte, Acta Cryst. B, vol. 55, 1999, pp. 563-572.
[73] S.J. Grabowski, J. Phys. Chem. A, vol. 105, 2000, pp. 5551-5557.
[74] L. Sobczyk, S.J. Grabowski, T.M. Krygowski, Chem. Rev., vol. 105, 2005, pp. 3513-3560.
[75] R.F.W. Bader, H. Essén, J. Chem. Phys., vol. 80, 1984, pp. 1943-1960.
[76] M.F. Bobrov, G.V. Popova, V.G. Tsirelson, Russ. J. Phys. Chem., vol. 80, 2006, pp. 584-590.
[77] E. Espinosa, I. Alkorta, J. Elguero, E. Molins, J. Chem. Phys., vol. 117, 2002, pp. 5529-5542.
[78] R.F.W. Bader, C.F. Matta, Inorg. Chem., vol. 40, 2001, pp. 5603-5611.
[79] R.F. Bader Journal (1990) Pages.
[80] S.M. Chemaly, M. Florczak, H. Dirr, H.M. Marques, Inorg. Chem., vol. 50, 2011, pp. 8719-8727.
[81] R.F. Pasternack, M.A. Cobb, J. Inorg. Nucl. Chem., vol. 35, 1973, pp. 4327-4339.
[82] R.F. Pasternack, M.A. Cobb, N. Sutin, Inorg. Chem., vol. 14, 1975, pp. 866-873.
[83] E.B. Fleischer, S. Jacobs, L. Mestichelli, J. Am. Chem. Soc,, vol. 90, 1967, pp. 2527-2531.

Figure(s)

Click here to download high resolution image

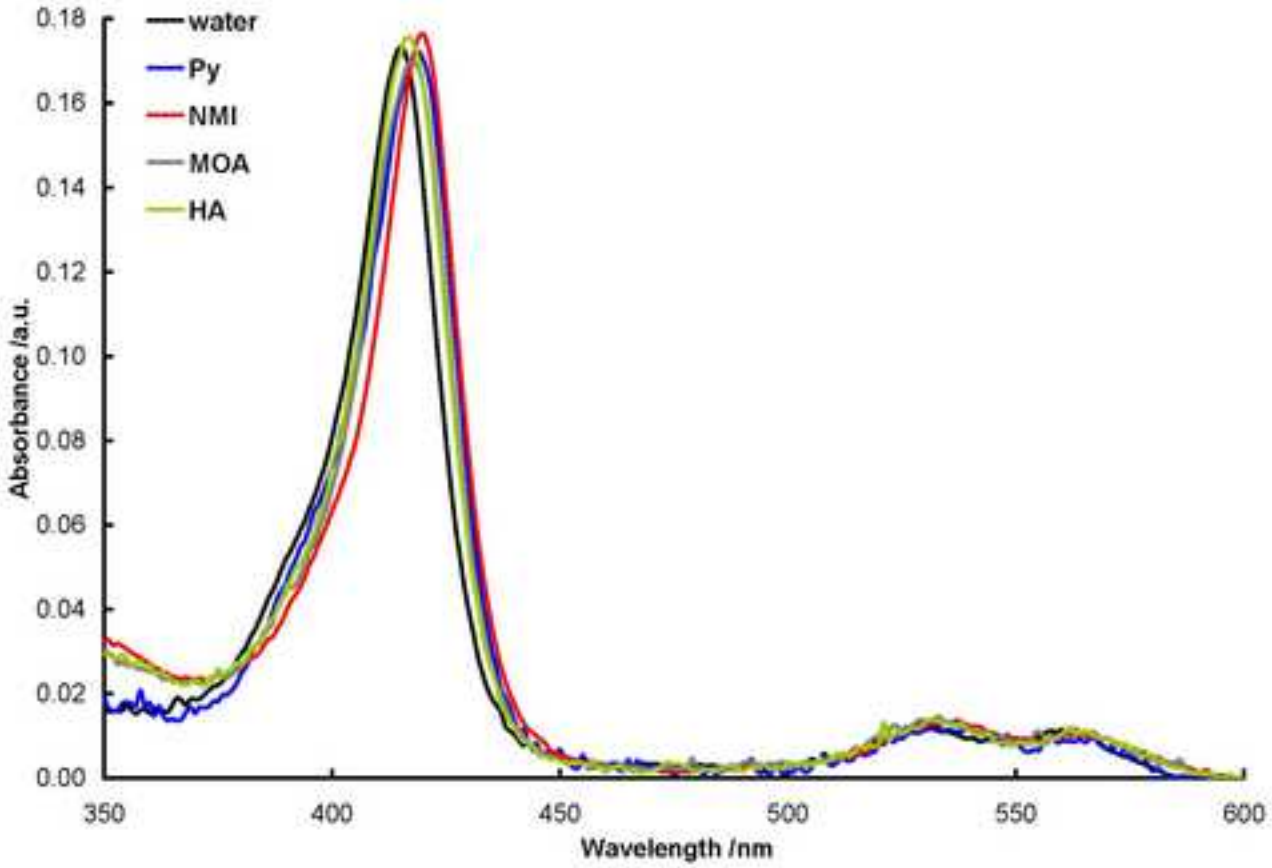

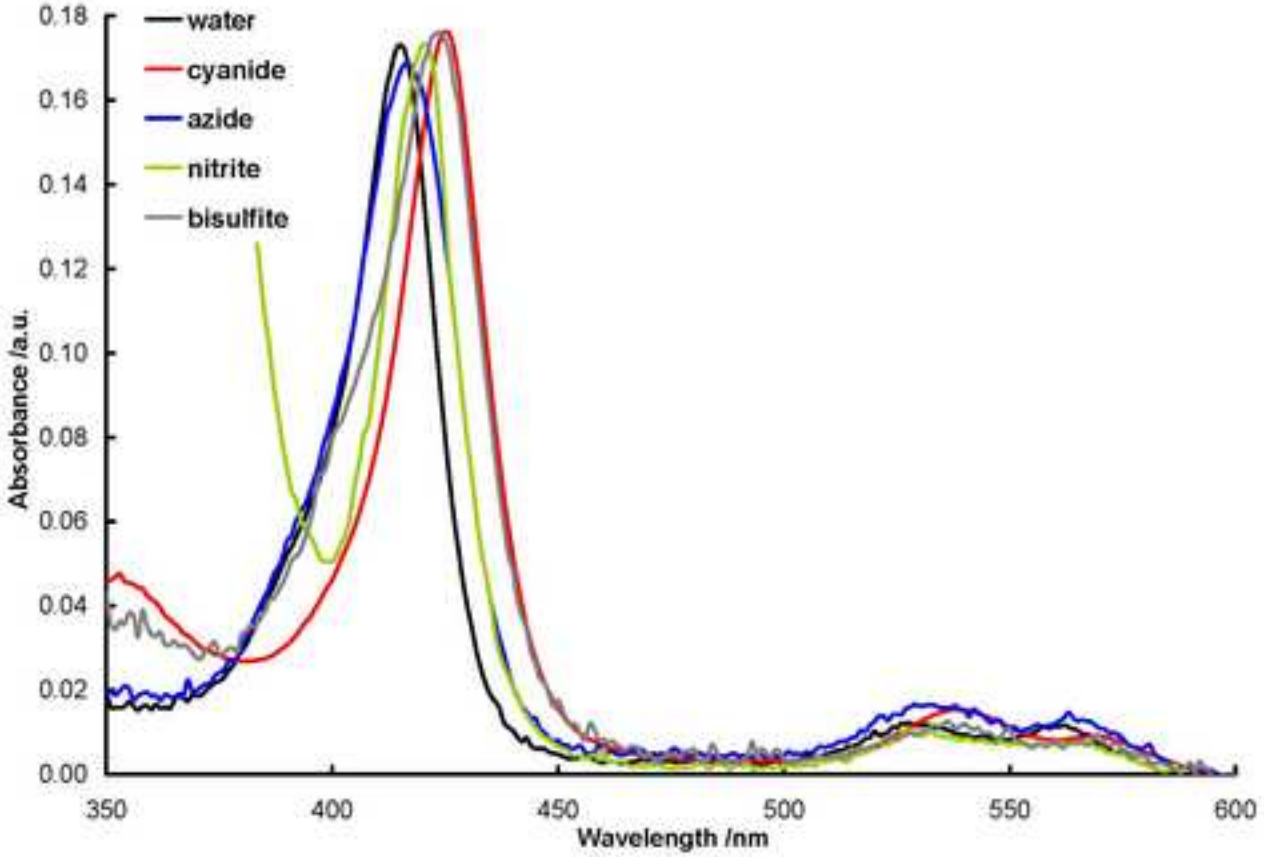

Figure(s)

Click here to download high resolution image

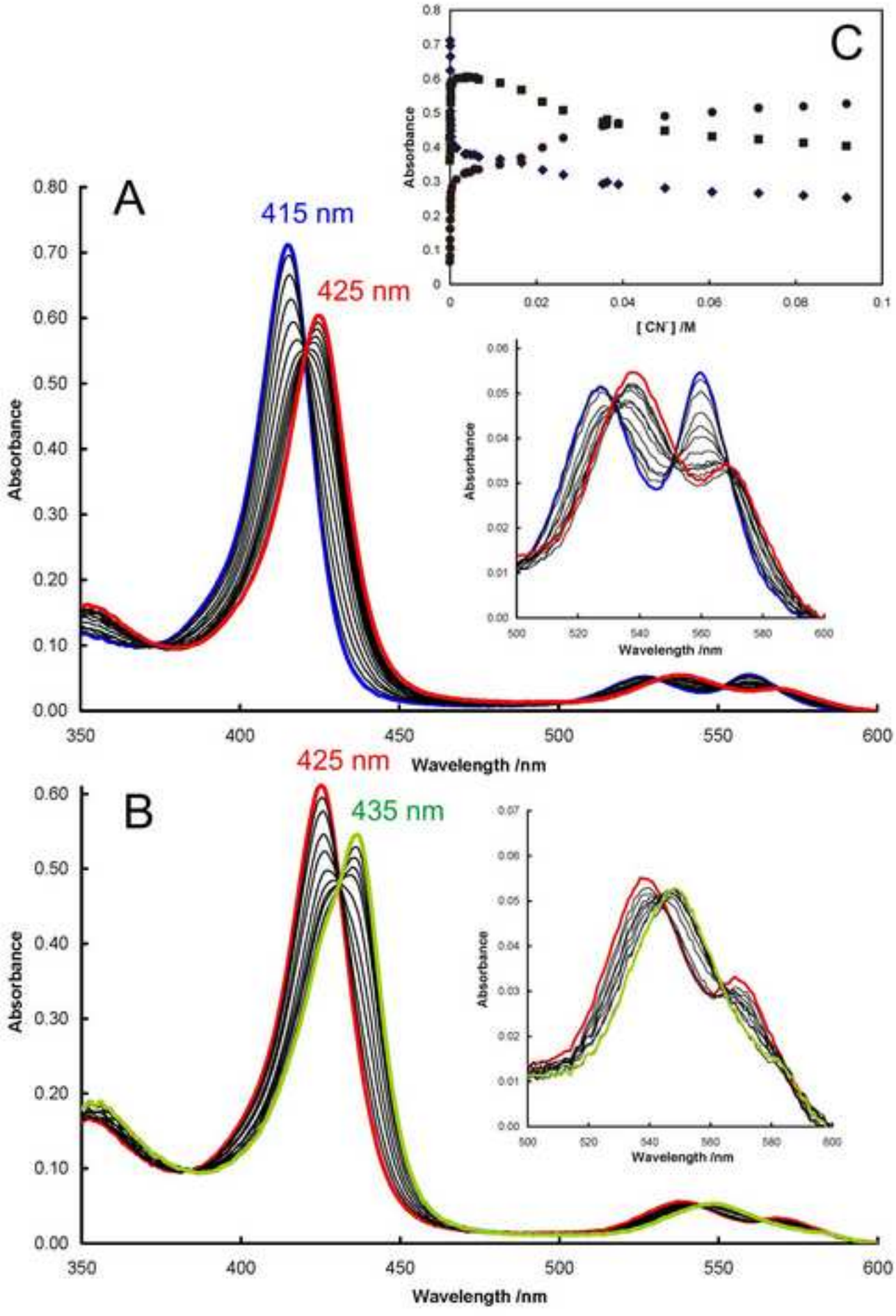

Figure(s)

Click here to download high resolution image

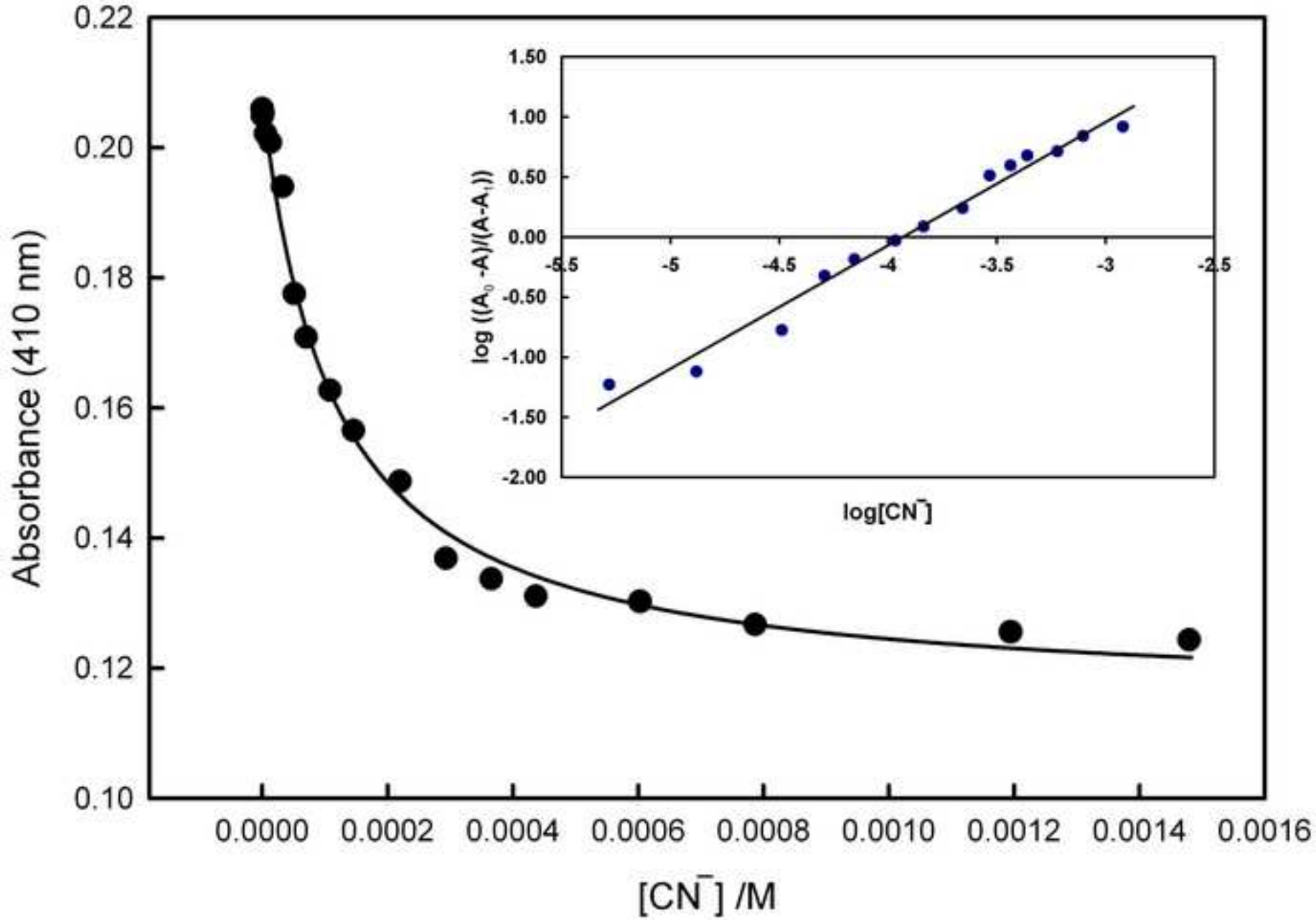

Figure(s)

Click here to download high resolution image

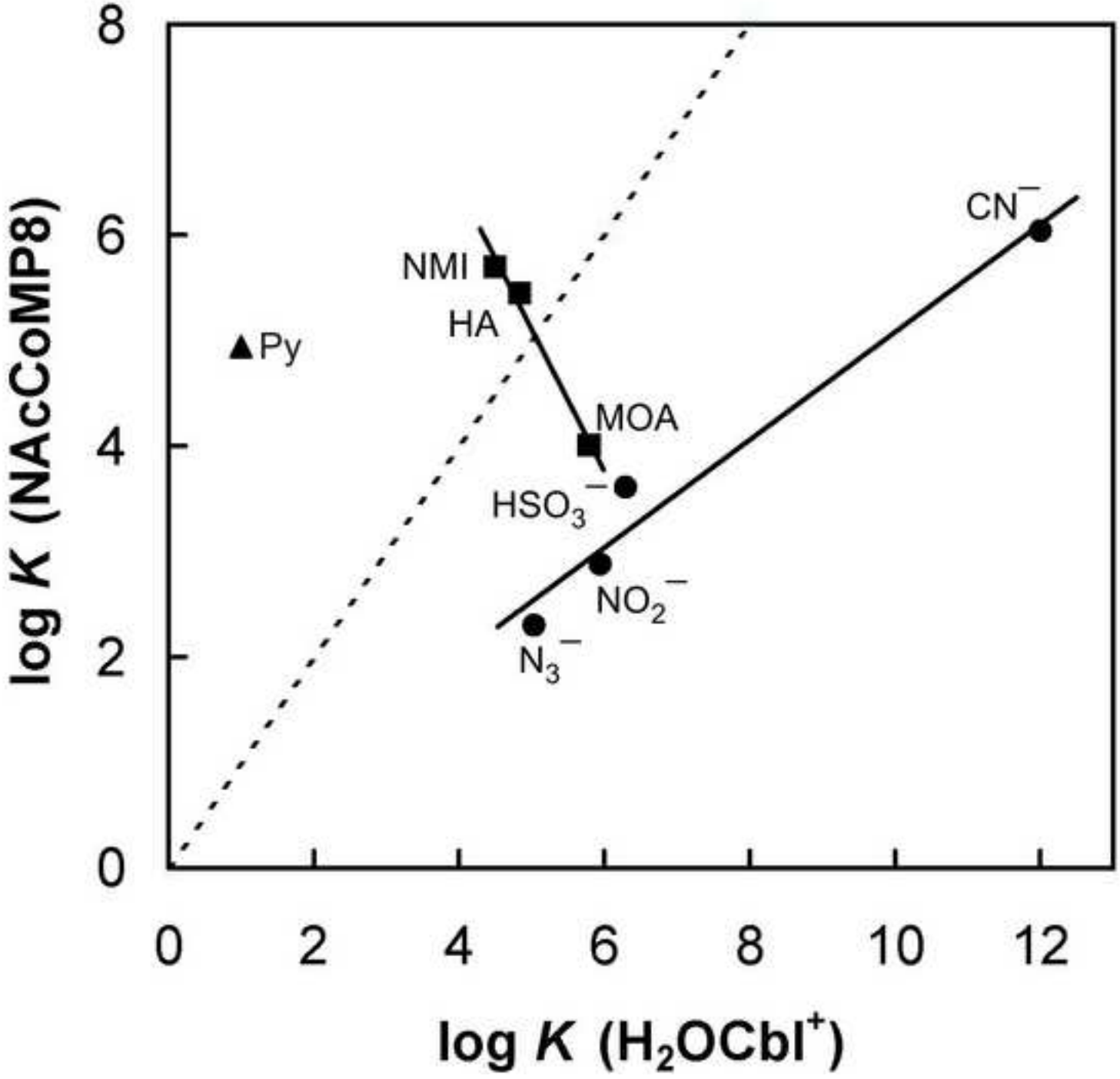

The Ligand Substitution Reactions of N-Acetyl-Co(III) Microperoxidase-8 (NAcCoMP8): a Comparison with Aquacobalamin (vitamin B_{12a})

Sadhna Mathura, Alvaro S. de Sousa, Christopher B. Perry, Isabelle Navizet and Helder M. Marques*

Molecular Sciences Institute, School of Chemistry, University of the Witwatersrand, P.O. Wits, Johannesburg, 2050 South Africa

Supplementary Information

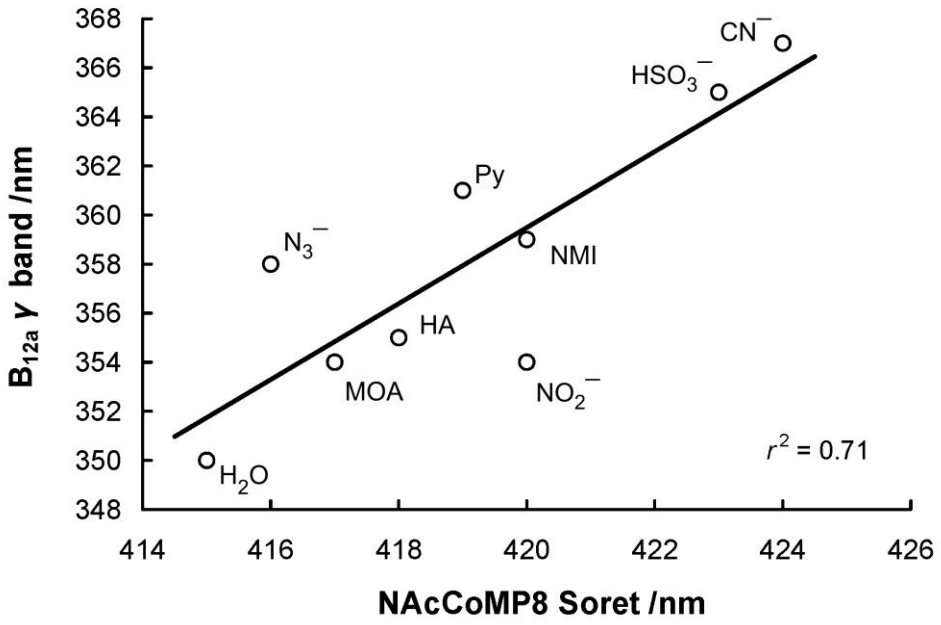

Figure S1. A comparison of the position of the Soret band in NAcCoMP8 and H_2OCbl^+ when H_2O is replaced by the indicated ligands. The trend indicates that both the corrin and porphyrin systems are sensitive to the donor power of the axial ligand. The softer ligands (HSO_3^-, CN^-) cause the greatest shift towards longer wavelength, consistent with a narrowing of the HOMO-LUMO gap of the delocalized π electron system of the macrocycles.

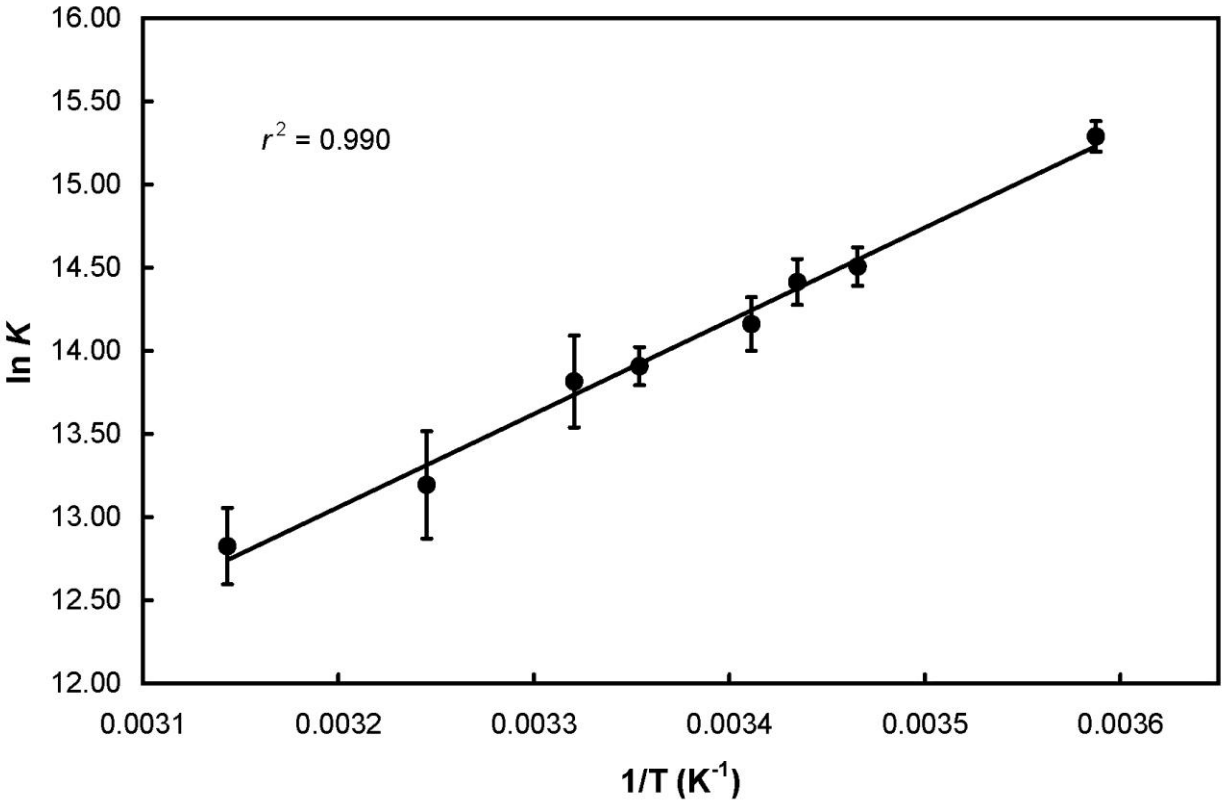

Figure S2. van't Hoff plot for the ligand substitution of H_2O by CN^- in NAcCoMP8. The straight line was fitted by weighted linear least squares methods.

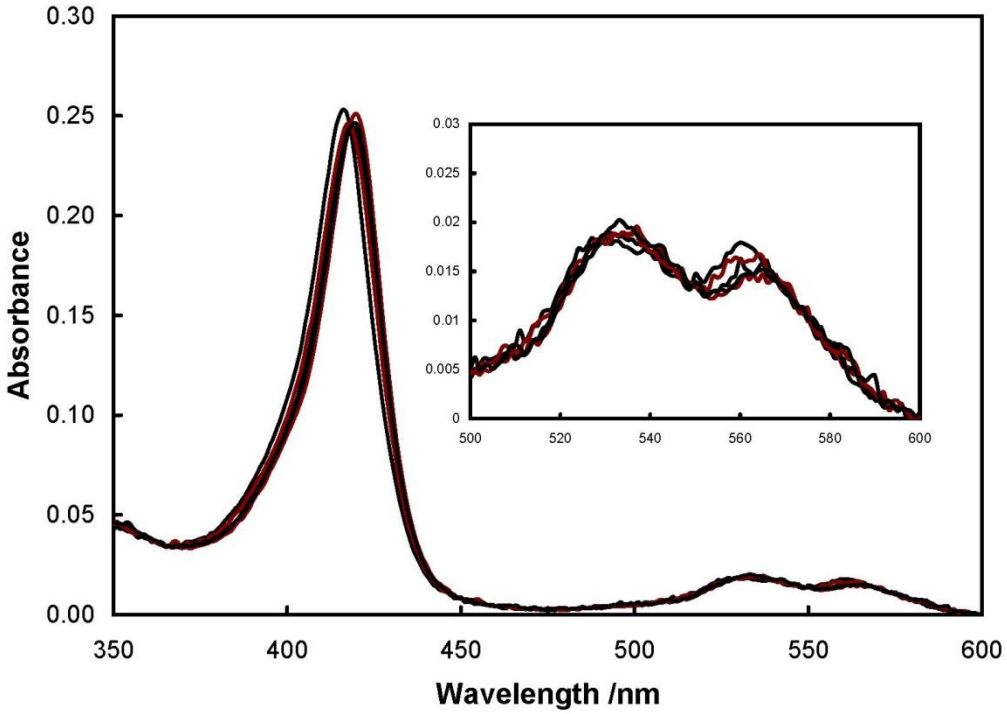

Figure S3. Spectroscopic changes observed during the titration of 1.55 μM NAcCoMP8 with NMI. The five spectra correspond to the addition of 0, 5.98, 11.9, 23.0 and 407 μM NMI (25 ^{o}C, pH 6.85, 0.1 M MOPS). The insert shows the very small spectroscopic changes in the visible region, making the data unusable. Binding isotherms were fitted to the absorbance changes between 390 and 415 nm, and between 418 and 435 nm at 1 nm intervals. The log *K* value reported is the weighted average of the log *K* value obtained from the weighted average of the K_{obs} values of the 44 fits.

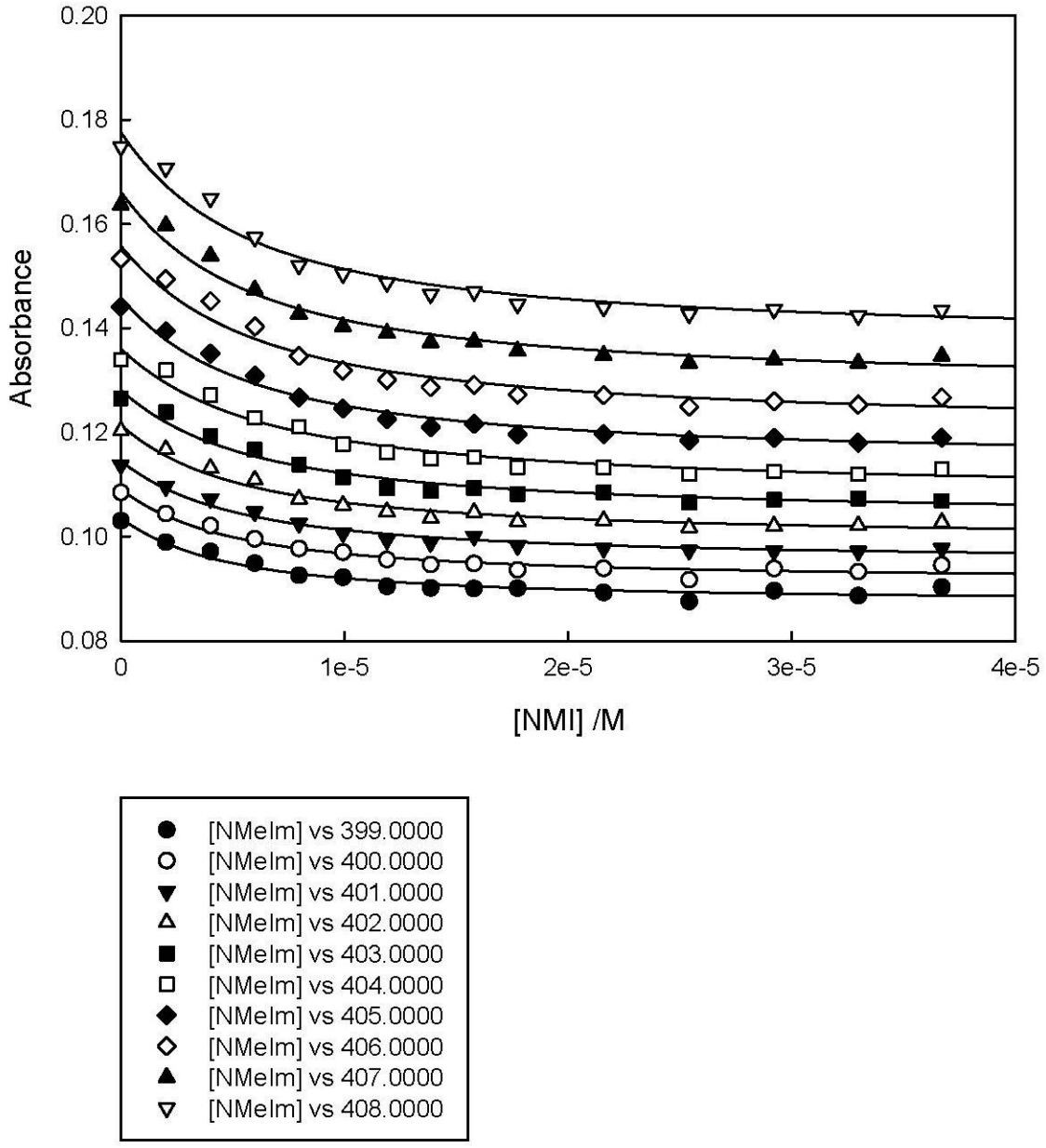

Figure S4. Examples of fits of eqn. 2 of the text, taking the free ligand concentration into account (eqn. 2) to the spectroscopic data obtained in the titration of NAcCoMP8 with NMI (25 ^{o}C, pH 6.85, 0.1 M MOPS, see Figure S2). Forty such fits yield a weighted average of log K = 5.76(8).

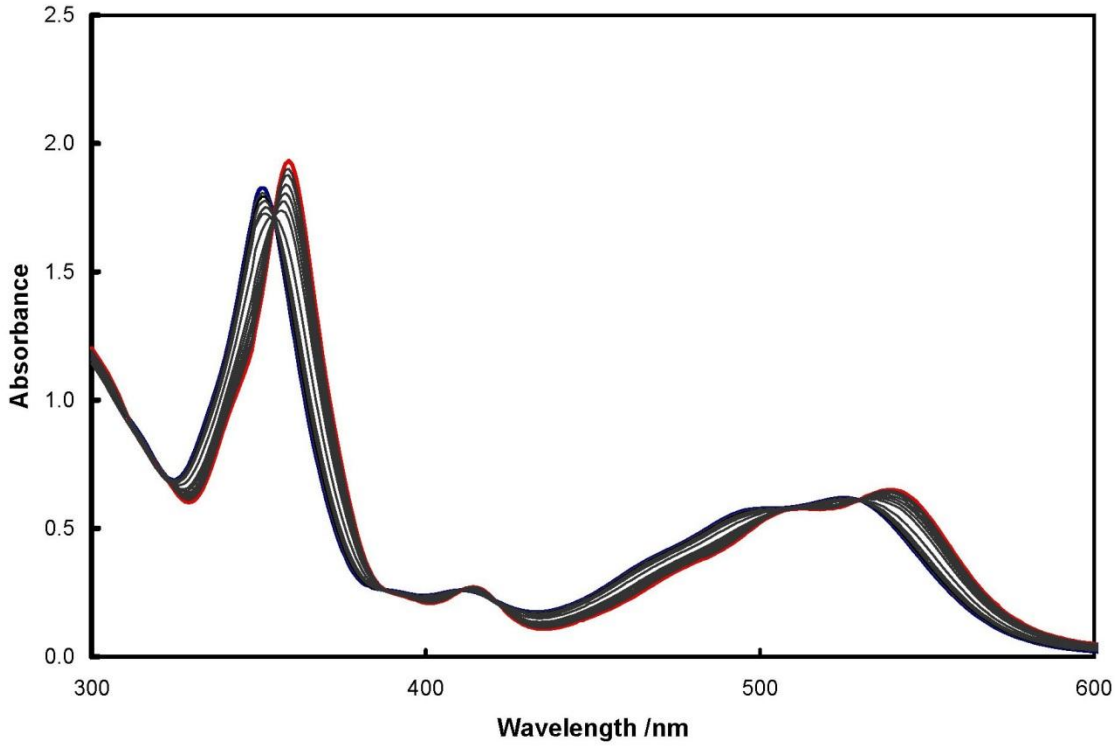

Figure S5. The substitution of H_2O in H_2OCbl^+ by NMI (up to 55.52 mM, pH 6.98, 0.1 M MOPS, 25 ^oC) proceeds with well-defined isosbestic points. A Hill plot (cf. insert to Figure 3 of the text) confirms the binding of a single ligand.

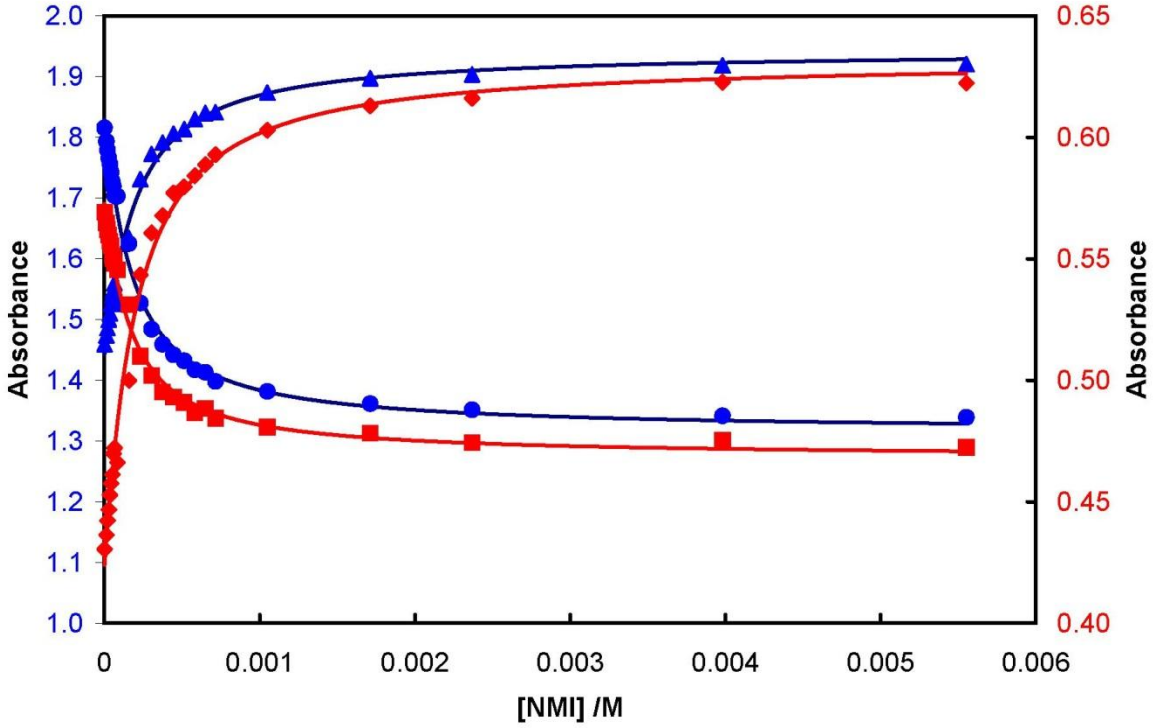

Figure S6. Fits of the absorbance data at 350 and 358 nm (blue circle and blue triangle, respectively, left axis) and at 495 and 545 nm (red square, red diamond, respectively, right axis) for displacement of H_2O by NMI in H_2OCbl^+ (Figure S5) to eqn. 2 of the text, taking the free ligand concentration into account (eqn. 3 of the text).

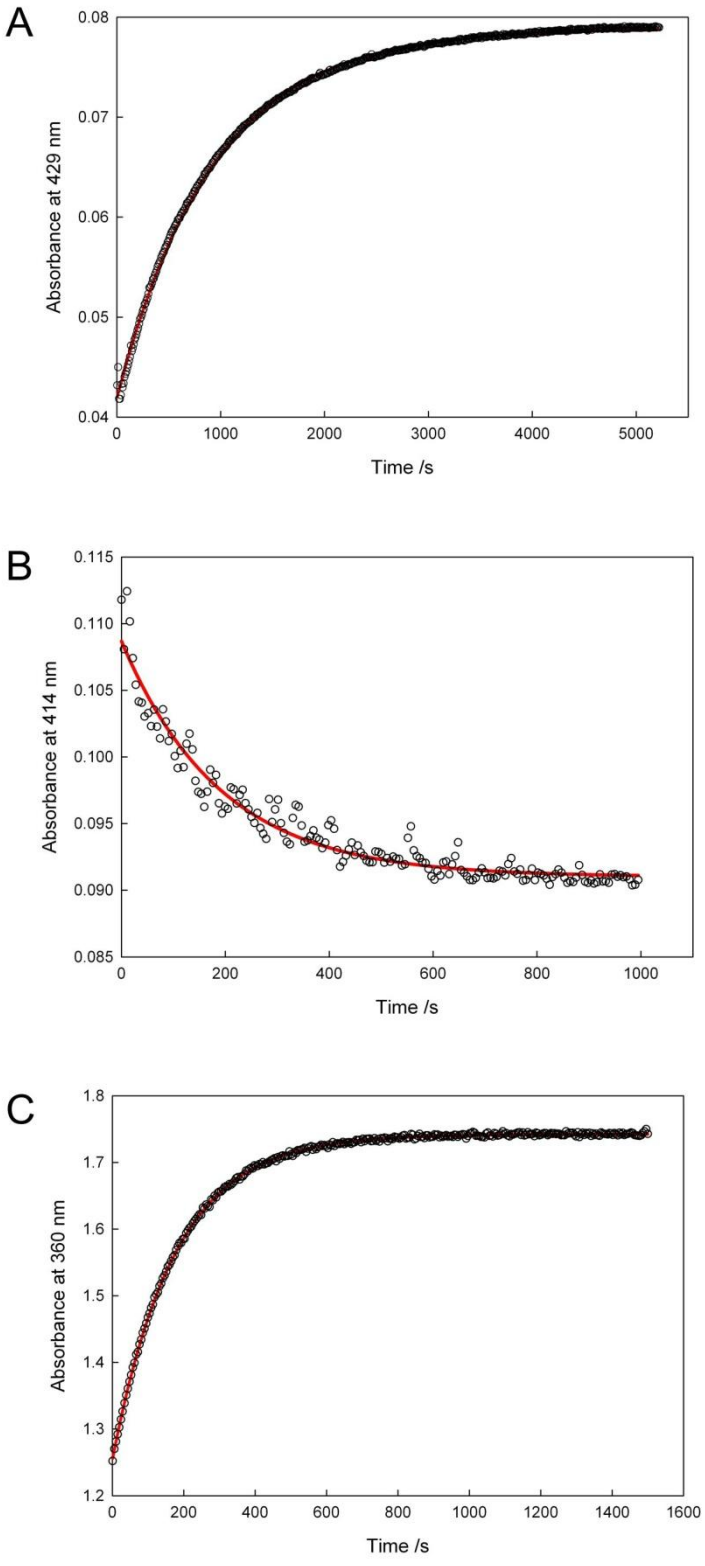

Figure S7. Fits to absorbance changes to an equation of the form $A = A_0 + A_1 e^{-k_I^{obs} t}$ for the reaction at 25 °C of (A) cyanide with NAcCoMP8, (B) NMI with NAcCoMP8 and (C) NMI with H_2OCbl^+. In (A): r^2 = 0.9995, k_I^{obs} = 1.08(3) × 10^{-3} s^{-1}, [CN^-] (corrected of pH) = 11.3 μM, pH 7.00. In (B): r^2 = 0.97, k_I^{obs} = 5.2(2) × 10^{-3} s^{-1}, [NMI] (corrected of pH) = 2.84 μM, pH 6.69. In (C): r^2 = 0.9996, k_I^{obs} = 5.71(2) × 10^{-3} s^{-1}, [NMI] (corrected for pH) = 334 μM, pH 6.88.

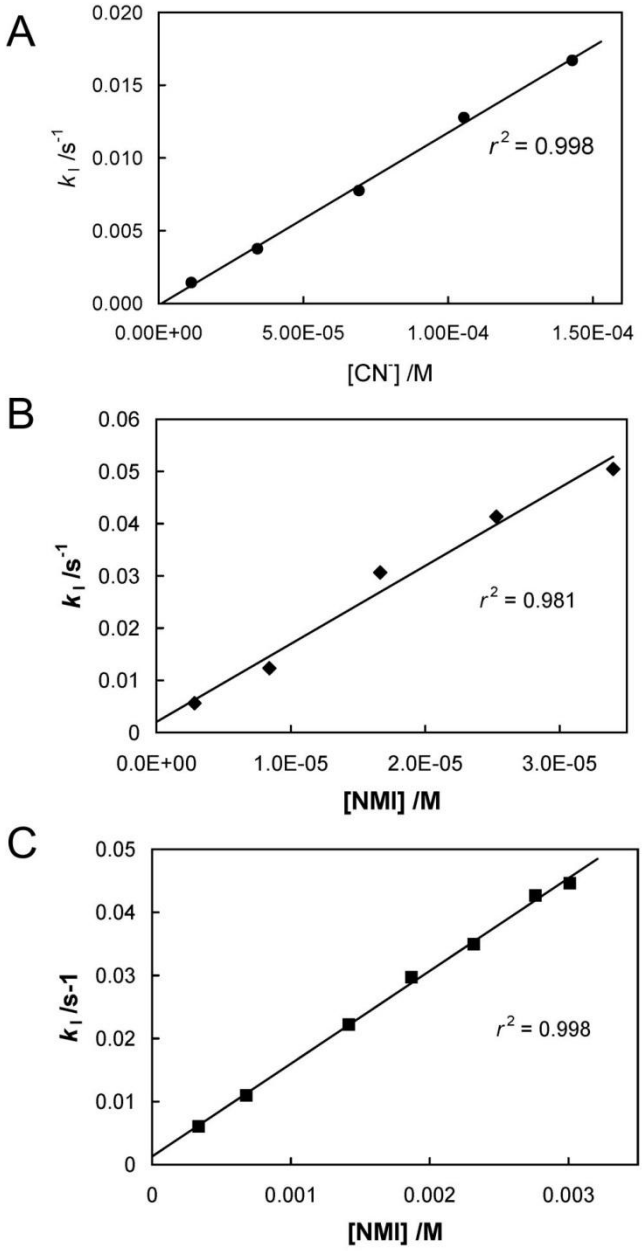

Figure S8. Plots of the pH-corrected pseudo first order rate constant, k_I, as a function of ligand concentration for the reaction at 25 ^oC of (A) CN^- with NAcCoMP8, (B) NMI with NAcCoMP8 and (C) NMI with H_2OCbl^+.

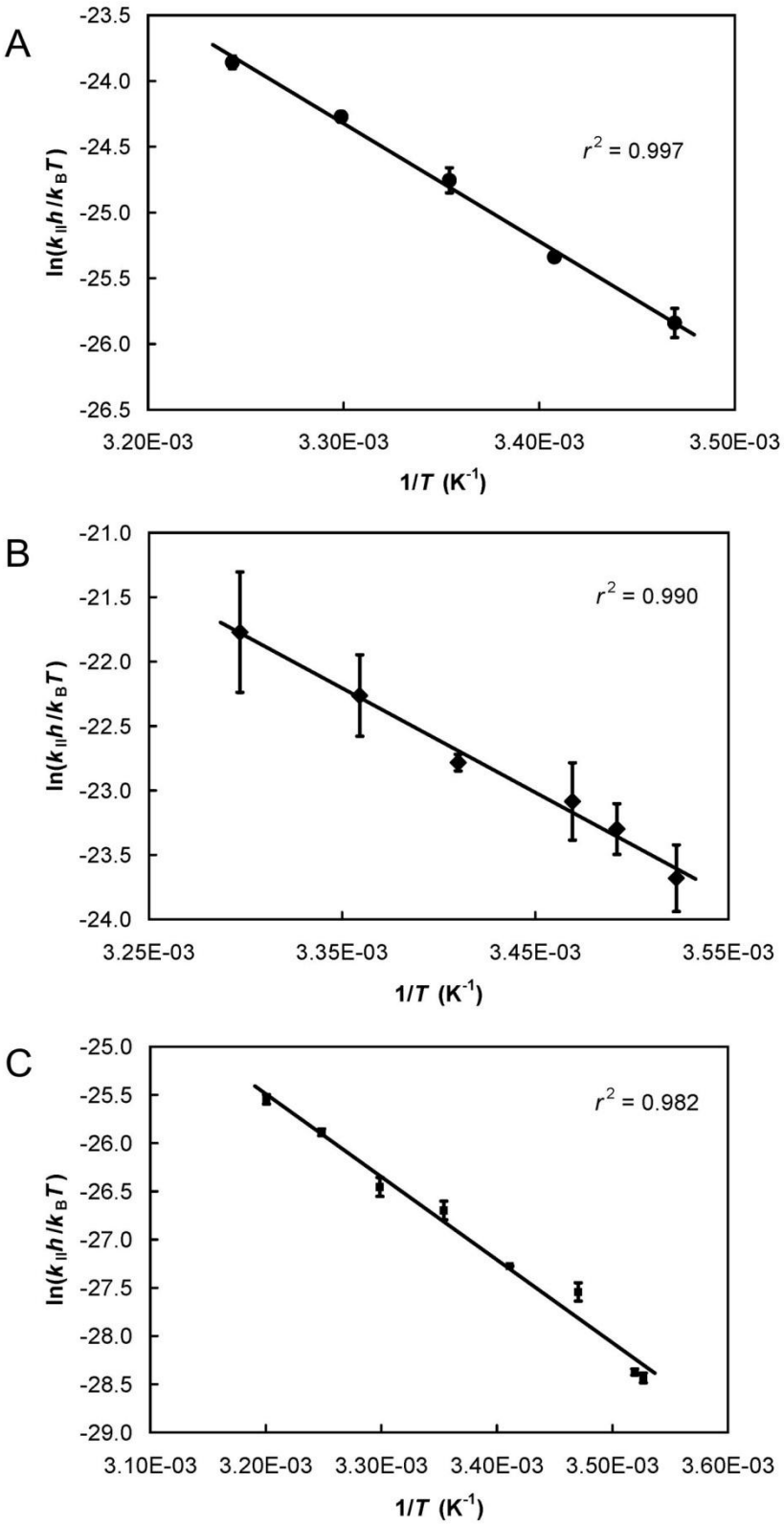

Fgure S9. Eyring plots for the reaction of (A) CN^- with NAcCoMP8, (B) NMI with NAcCoMP8 and (C) NMI with H_2OCbl^+.

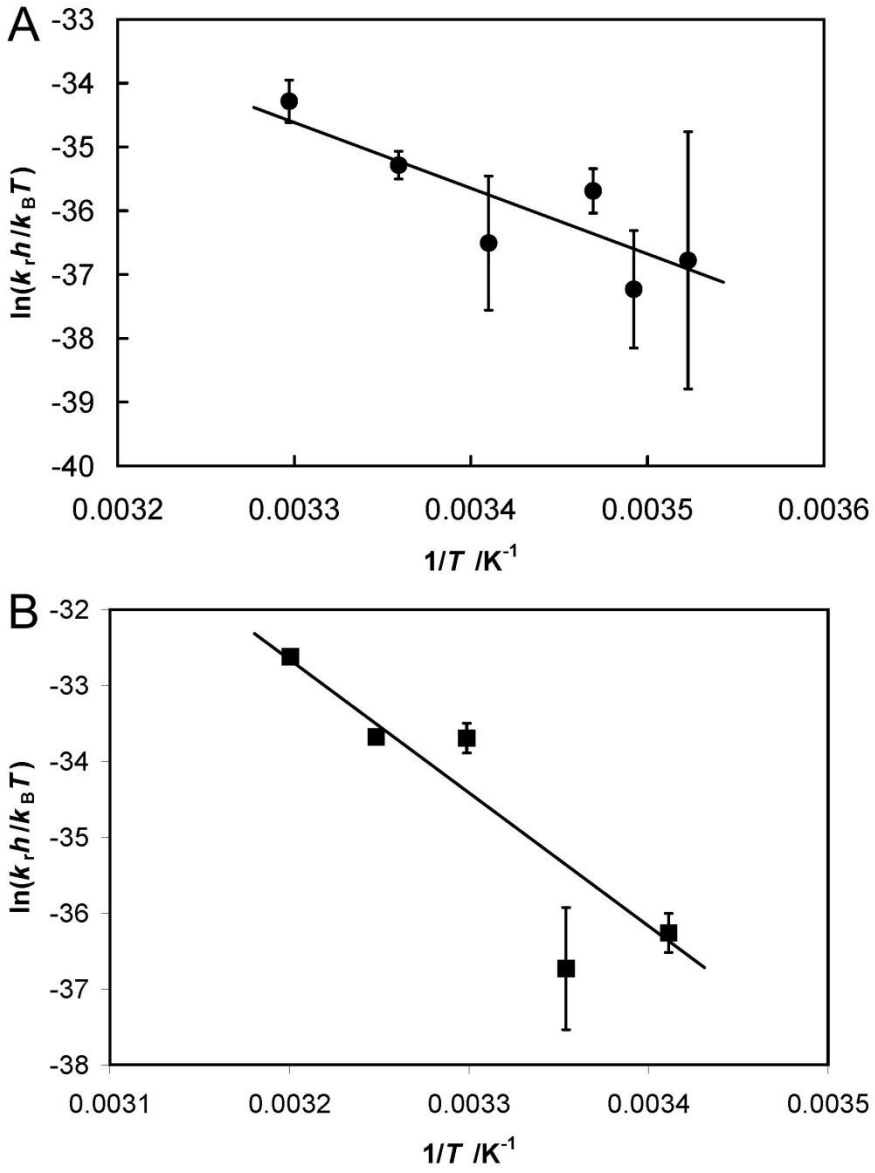
A
-33
-34
-35
-36
-37
-38
-39
-40
ln(k_r h/k_B T)
0.0032
0.0033
0.0034
0.0035
0.0036
1/T /K^-1
B
-32
-33
-34
-35
-36
-37
-38
ln(k_r h/k_B T)
0.0031
0.0032
0.0033
0.0034
0.0035
1/T /K^-1

Figure S10. Eyring plots for the reverse reaction of NMI with (A) NAcCoMP8 and (B) with H_2OCbl^+. The reverse rate constants are from the intercepts of plots such as in Figure S12 B and C. In the case of the reaction of NMI with H_2OCbl^+ the intercepts were not statistically different from zero for reactions at $T < 20\ ^oC$ and the data were omitted from the plot in (B).

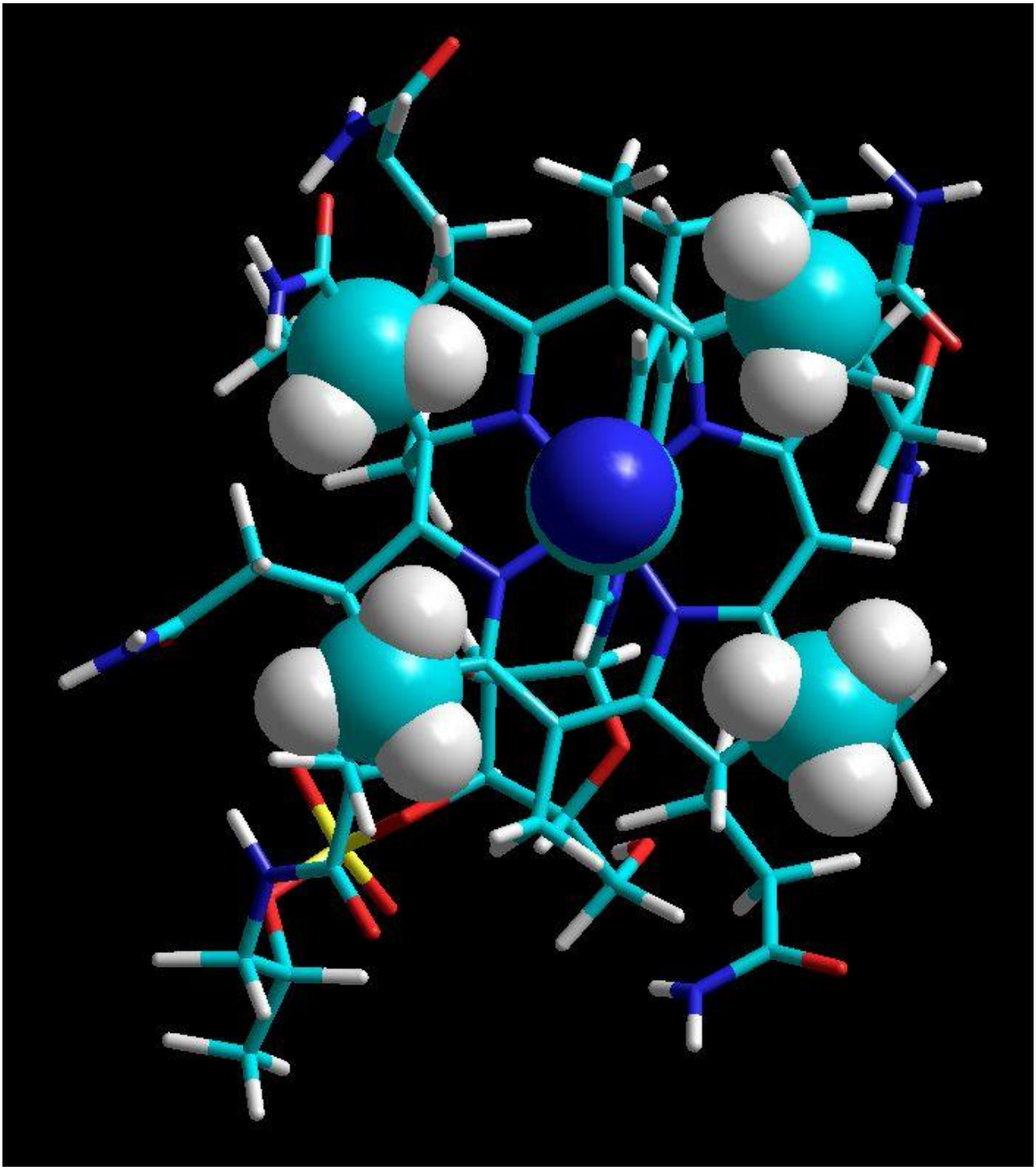

Figure S11. A view from the upper or β face of the corrin in cyanocobalamin showing the sentinel-like effect of the methylene groups of C26 and C37 of the *a* and *c* side chains, respectively, and methyl groups C46 and C54. Adapted from the crystal structure of cyanocobalamin [1].

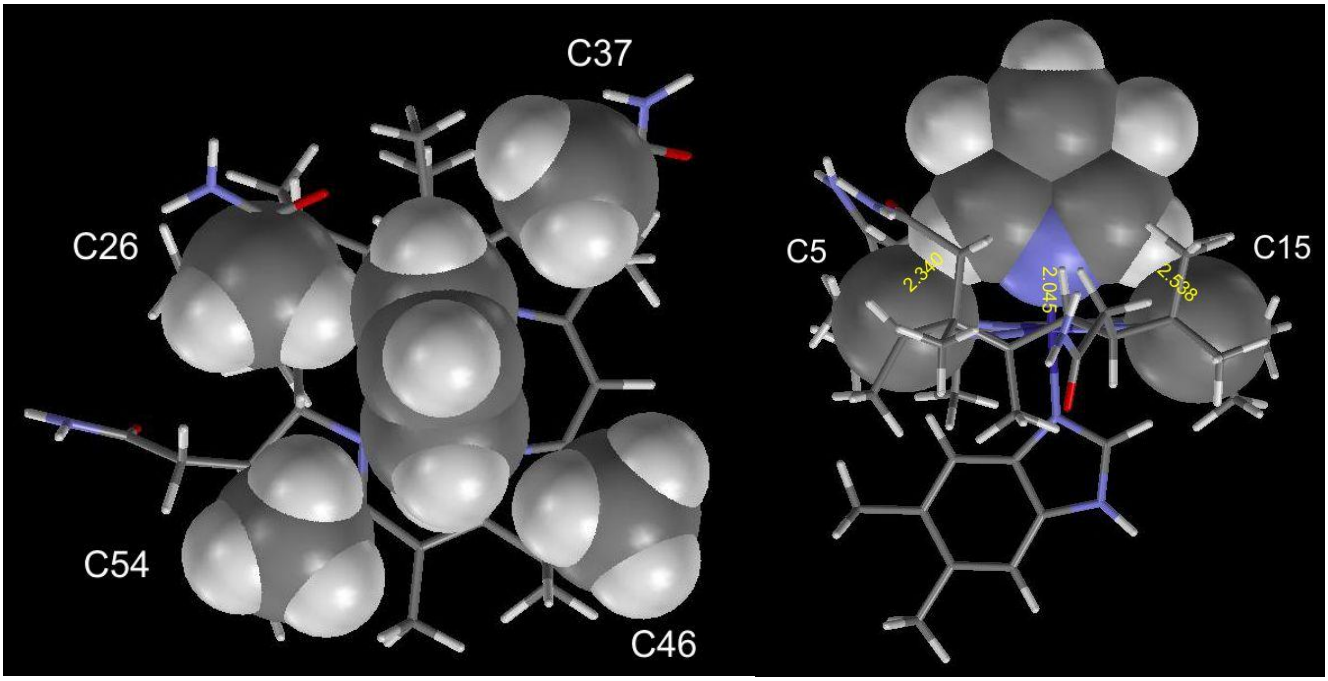

Figure S12. The DFT geometry-optimized structure of a model of $PyCbl^+$. (a) View from the upper (β) face of the corrin showing how Py is constrained by the sentinel substituents of the corrin (left). (b) View from the C1–C19 bond of the corrin showing the van der Waals contact between the H atoms of the α carbon atoms of Py with C5 and C15 (right). All distances in Å.

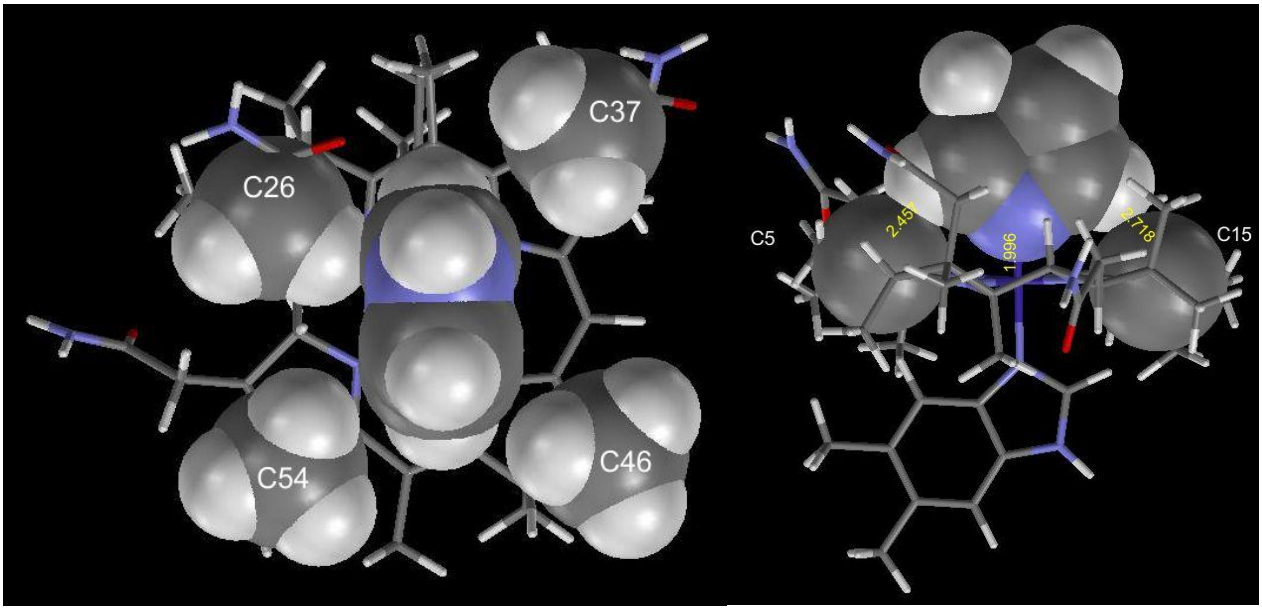

Figure S13. The DFT geometry-optimized structure of a model of $imidazoleCbl^+$. (a) View from the upper (β) face of the corrin showing how imidazole, like Py (Figure S9) is constrained by the sentinel substituents of the corrin (left). (b) View from the C1–C19 bond of the corrin showing the van der Waals contact between the H atoms of the α carbon atoms of imiazdole with C5 and C15 (right). All distances in Å. The Co–$N_{imidazole}$ bond length is shorter than that to Py, and although the α hydrogen atoms still come into van der Waals contact with C5 and C15, they are further away than in Py.

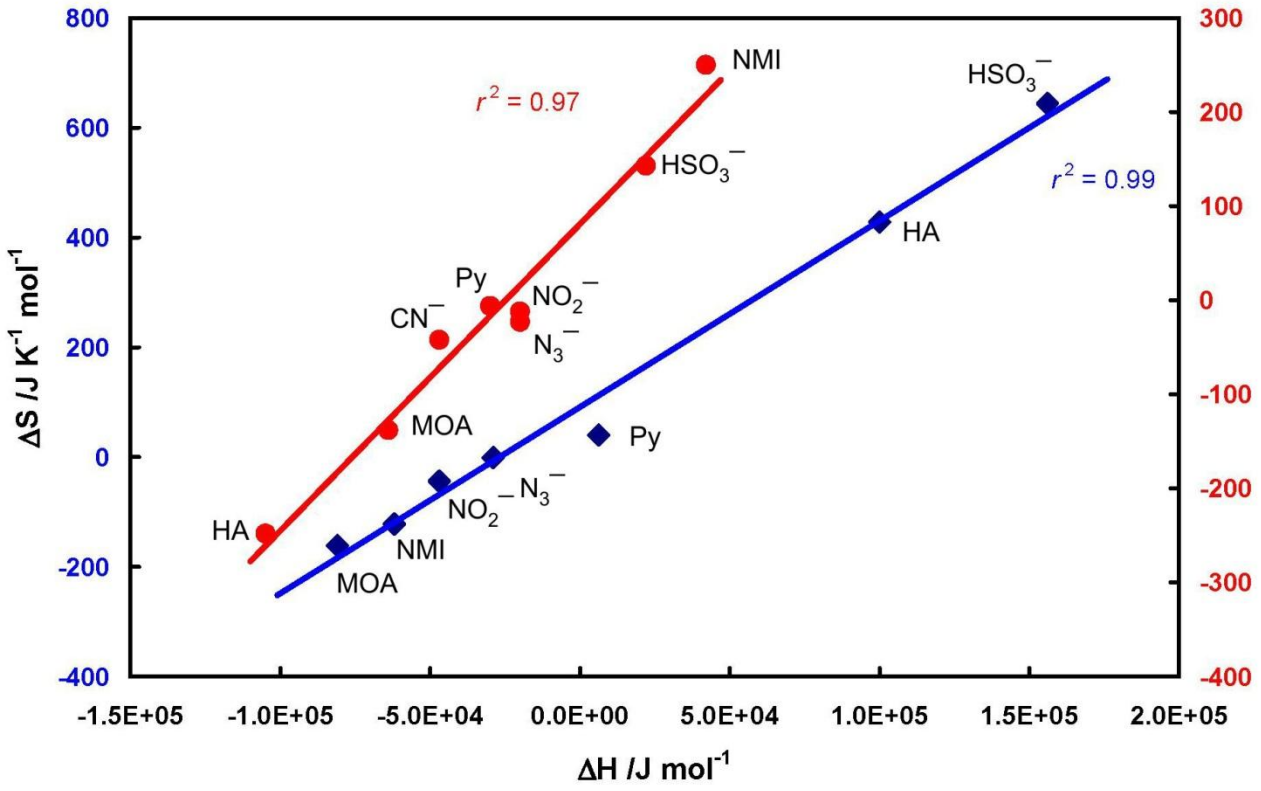

Figure S14. Correlation between Δ*H* and Δ*S* for the substitution of coordinated H_2O in H_2OCbl^+ (blue, left axis) and in NAcCoMP8 (red, right axis) by neutral and anionic ligands.

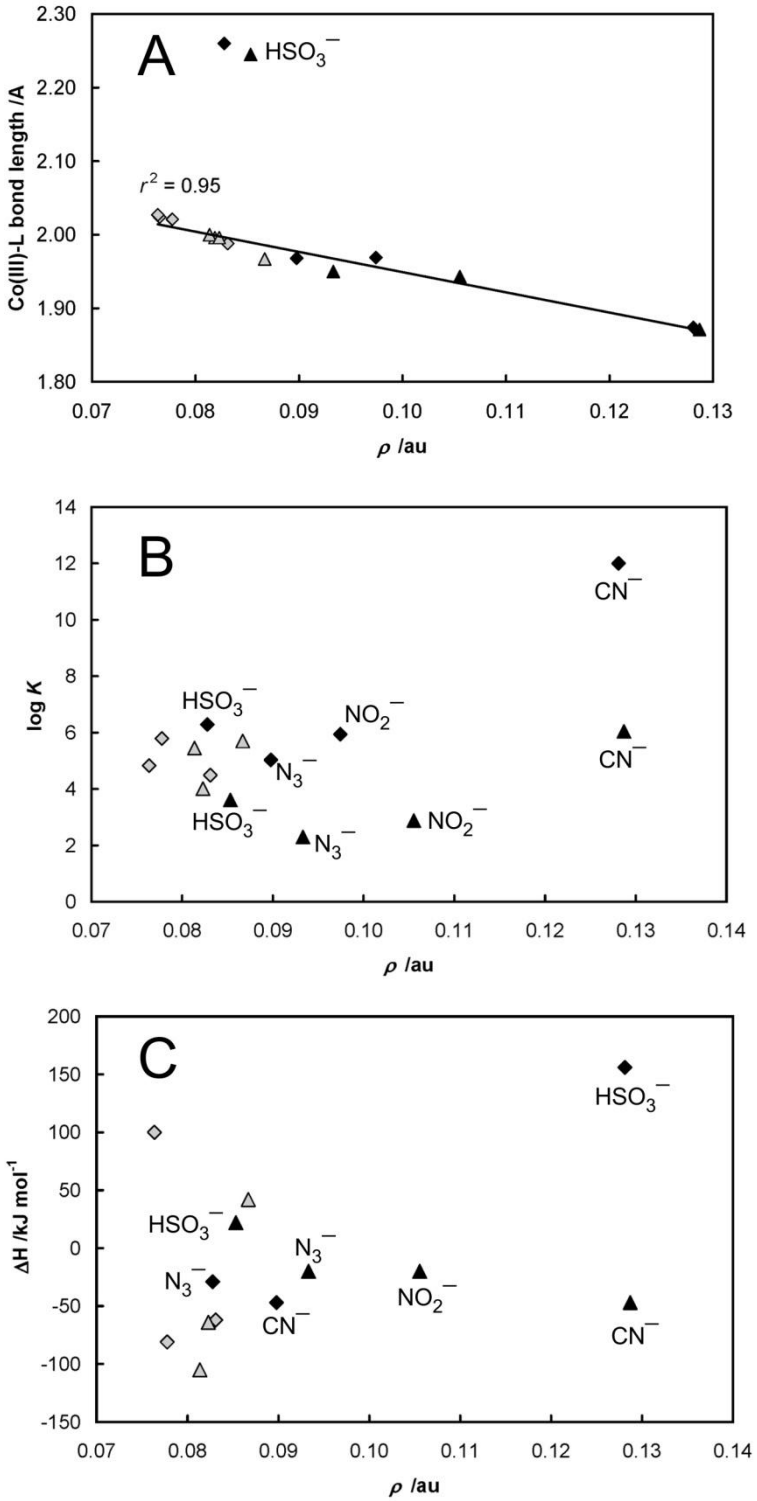

Figure S15. (A) The bond length between Co(III) and an axial ligand correlates with the electron density, ρ, at the bond critical point for anionic ligands on a corrin (black diamond), neutral ligands on corrin (grey diamonds), anionic ligands on a porphyrin (black triangles) and neutral ligands on a porphyrin (grey triangles) provided the value for the S donor, HSO_3^-, is omitted because of its much larger radius. There is no significant correlation between ρ can log K (B) or ΔH (C) for coordination of the ligands by the Co(III) complexes.

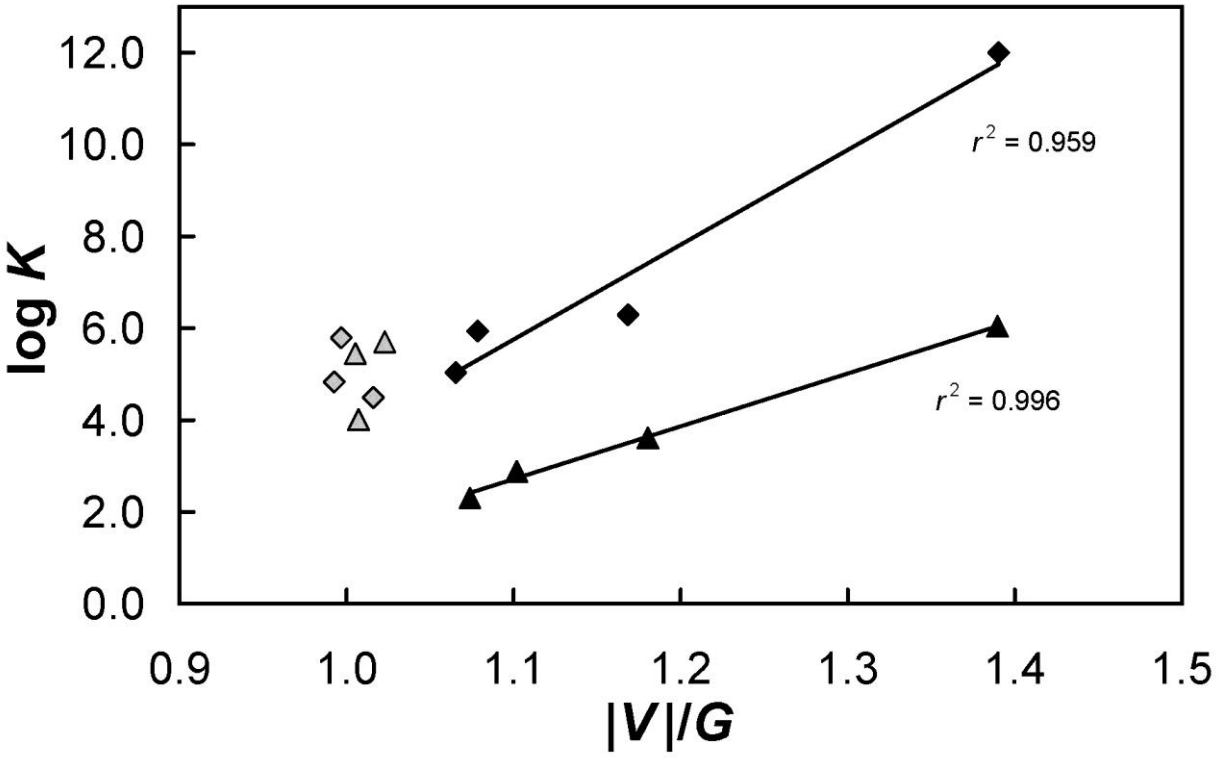

Figure S16. Correlation between log *K* for the binding of anionic ligands L by H_2OCbl^+ (filled diamonds) and NAcCoMP8 (filled triangles) and the ratio of the potential and kinetic energy densities at the Co–L bond critical point obtained from a QTAIM analysis of the electron density. There is no correlation for the bind of neutral ligands (open diamonds and triangles, respectively).

Table S1. Bond lengths between Co(III) and N of pyridine in a variety of complexes in which the equatorial ligand(s) provide four N donors to the metal, and the trans ligand is also an N donor.

CSD Refcode	Co-N(1)	Co-N(2)		Trans ligand	Ref
Cobaloximes					
CIHXAT	2.050	2.050		py	[2]
HAWTAB	1.968	1.956		py	[3]
HEPHIT	2.004	2.004		py	[4]
JOSREO	1.982	1.982		py	[5]
LACHAZ	1.964	1.984		py	[6]
METJEB	1.965	1.965		py	[7]
SOMNEN	1.956	1.989		py	[8]
	Mean	*1.99*			
	σ	*0.03*			
Corroles					
GEDQEM	1.981	2.004		py	[9]
GEDQIQ	1.998	1.998		py	[9]
MEWMUW	1.976	1.979		py	[10]
NALFOW	1.969	1.978		py	[11]
TIJBAP	1.994	1.995		py	[12]
TIJBET	1.990	2.000		py	[12]
	Mean	*1.99*			
	σ	*0.02*			
Aliphatic					
SAYLAF	1.976		$[Co(en)_2(py)(NH_3)]^{3+}$	NH_3	[13]
AMMNPCO	1.960		$[Co(NH_3)_4(py)(NO_2)]^{2+}$	NO_2^-	[14]
GADSOT	1.966		$[Co(NH_3)_5(py)]^{3+}$	NH_3	[15]
	Mean	*1.97*			
	σ	*0.01*			
Porphyrins					
EBOMAK	1.970	1.959		py	[16]
YEQMIQ	2.032			NO_2^-	[17]
YEQMUM	2.044			NO_2^-	[17]
NTPOLC	2.037			NO_2^-	[18]
	Mean	*2.01*			
	σ	*0.04*			

Table S2. Bond lengths and ρ_b for the axial bonds in modeled (M06L/SVP/SVPFit) corrin and porphyrin structures (L–Co(N_4)–Im), N_4 = porphyrin or corrin

L	**Corrin**				**Porphyrin**			
	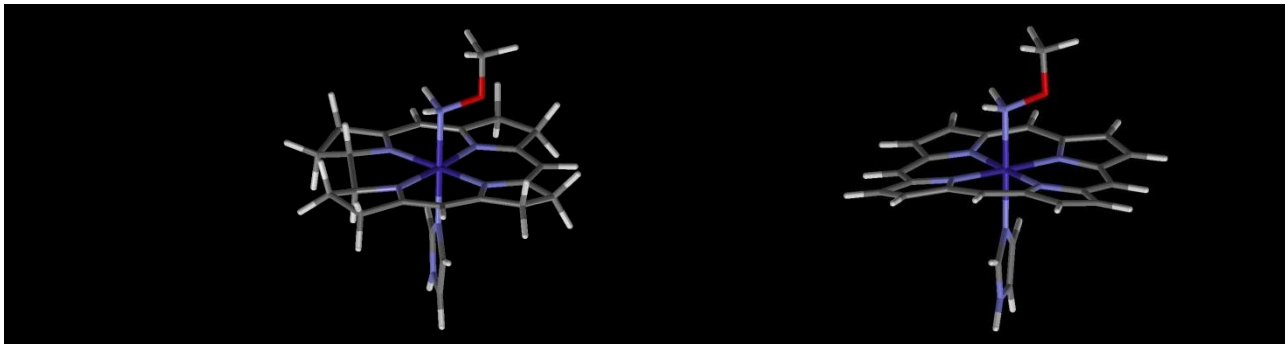							
	Co–L /Å	**Co–Im /Å**	**ρ_b Co–L /au**	**ρ_b Co–Im /au**	**Co–L /Å**	**Co–Im /Å**	**ρ_b Co–L /au**	**ρ_b Co–Im /au**
NH_3	2.024	1.969	0.07654	0.08733	1.996	1.952	0.08187	0.09012
NH_2OH	2.027	1.966	0.07636	0.08828	2.000	1.949	0.08136	0.09119
NH_2OMe	2.021	1.968	0.07776	0.08767	1.996	1.950	0.08229	0.09079
Im	1.988	1.988	0.08311	0.08312	1.967	1.968	0.08664	0.08668
CN^-	1.874	2.077	0.12810	0.06536	1.871	2.071	0.12870	0.06563
NO_2^-	1.969	2.078	0.09742	0.06623	1.934	2.075	0.10553	0.06583
HSO_3^-	2.260	2.054	0.08278	0.07050	2.247	2.067		
N_3^-								

Table S3. Topological properties at the bond critical points of the axial ligands of L–Co(III)(N_4)–Im complexes (N_4 = equatorial corrin or porphyrin from a DFT model (M06L/SVP/SVPFit).[a]

L	ρ	$\nabla^2\rho$	H	$\lvert V\rvert/G$	λ_1	λ_2	λ_3	ε	DI(Co,L)			
N-C(Im) [b]	0.29864	-0.52691	-0.47727	2.38122	-0.58123	-0.50532	0.55965	0.15021	1.0721			
C-C(Im) [b]	0.32086	-0.80048	-0.31925	3.67987	-0.66294	-0.48405	0.34652	0.36957	1.4389			
Corrin												
	ρ	$\nabla^2\rho$	H	$\lvert V\rvert/G$	λ_1	λ_2	λ_3	ε	DI(Co,L)	q(Co)	q(N_{im})	q(L)
NH_3	0.07654	0.43750	0.00023	0.99791	-0.06996	-0.06787	0.57533	0.03080	0.5017	1.3889	-1.1920	-1.2637
NH_2OH	0.07636	0.44768	0.00083	0.99254	-0.07259	-0.06747	0.58534	0.04054	0.4808	1.3842	-1.2628	-0.5869
NH_2OMe	0.07776	0.45186	0.00036	0.99680	-0.07259	-0.06999	0.59444	0.03718	0.4882	1.3855	-1.2634	-0.5838
Imidazole	0.08311	0.47048	-0.00191	1.01598	-0.07982	-0.07695	0.62725	0.03721	0.5216	1.4013	-1.2642	-1.2638
CN^-	0.12810	0.29014	-0.04643	1.39029	-0.15809	-0.15488	0.60311	0.02072	0.8031	1.3336	-1.2713	0.8162
NO_2^-	0.09742	0.41929	-0.00892	1.07846	-0.12857	-0.12071	0.66857	0.06505	0.5778	1.3404	-1.2664	0.5583
HSO_3^-	0.08278	0.22894	-0.01160	1.16848	-0.08335	-0.08147	0.39376	0.02317	0.5855	1.2732	-1.2646	2.5821
N_3^-	0.08978	0.40712	-0.00711	1.06531	-0.10466	-0.09938	0.61116	0.05307	0.5867	1.3789	-1.2642	-0.3082
Porphyrin												
	ρ	$\nabla^2\rho$	H	$\lvert V\rvert/G$	λ_1	λ_2	λ_3	ε	DI(Co,L)	q(Co)	q(N,im)	q(L)
NH_3	0.08187	0.47119	-0.00129	1.01082	-0.07684	-0.07541	0.62344	0.01896	0.5255	1.4063	-1.1896	-1.2599
NH_2OH	0.08136	0.47858	-0.00063	1.00525	-0.07726	-0.07627	0.63210	0.01298	0.5044	1.3990	-1.2585	-0.5856
NH_2OMe	0.08229	0.48466	-0.00087	1.00715	-0.07827	-0.07618	0.63911	0.02735	0.5081	1.3996	-1.2589	-0.5847
Imidazole	0.08668	0.50051	-0.00293	1.02288	-0.08398	-0.08101	0.66549	0.03667	0.5338	1.4188	-1.2565	-1.2568
CN^-	0.12870	0.29201	-0.04660	1.38961	-0.15815	-0.15719	0.60736	0.00606	0.8223	1.3492	-1.2610	0.8367
NO_2^-	0.10553	0.45778	-0.01298	1.10185	-0.14623	-0.13314	0.73715	0.09835	0.6205	1.3564	-1.2577	0.5621
HSO_3^-	0.08532	0.22662	-0.01247	1.18035	-0.08923	-0.08671	0.40256	0.02910	0.6097	1.2767	-1.2564	2.6128
N_3^-	0.09331	0.42756	-0.00852	1.07385	-0.11075	-0.10397	0.64229	0.06521	0.6161	1.3966	-1.2556	-0.2969

[a]All values in au; 1 au of ρ = 6.7483 e Å^{-3}; 1 au of $\lambda_{1,2,3}$ = 24.099 e Å^{-5}; 1 au of $\nabla^2\rho$ = 24.099 e Å^{-5}; 1 au of energy density (V, G, H) = 627.5095 kcal mol^{-1}. [b]For reference, topological properties of the electron density of one N–C and one C–C bond of axial imidazole are given.

References

[1] B. Dittrich, T. Koritsanszky, A. Volkov, S. Mebs and P. Luger, Angew. Chem., Int. Ed., 46 (2007) 2935.
[2] D. Mandal, M. Bhuyan, M. Laskar and B. D. Gupta, Organometallics, 26 (2007) 2795.
[3] S. Ozturk, M. Akkurt, M. Macit, S. Isik and H. K. Fun, Molecules, 10 (2005) 767.
[4] Y. M. Chumakov, V. N. Biuyshkin, V. I. Tsapkov, M. V. Gandzii, N. M. Samus and T. I. Malinovskii, Koord. Khim., 19 (1993) 714.
[5] D. Xu, L. Lei, Y. Zu, C. Cheng and J. Chen, Acta Crystallogr. Sec. C., 48 (1992) 1399.
[6] P. N. Bourosh, E. B. Koropceanu, Y. A. Simonov, O. A. Bologa and N. V. Gerbeleu, Koord. Khim., 28 (2002) 689.
[7] J. Gradinaru, S. Malinovskii, M. Gdaniec and S. Zecchin, Polyhedron, 25 (2006) 3417.
[8] A. Abusamleh, P. J. Chmielewski, P. R. Warburton, L. Morales, N. A. Stephenson and D. H. Busch, J. Coord. Chem., 23 (1991) 91.
[9] N. Maiti, J. Lee, S. J. Kwon, J. Kwak, Y. Do and D. G. Churchill, Polyhedron, 25 (2006) 1519.
[10] R. Guilard, F. Jerome, J.-M. Barbe, C. P. Gros, Z. Ou, J. Shao, J. Fischer, R. Weiss and K. M. Kadish, Inorg.Chem., 40 (2001) 4856.
[11] J.-M. Barbe, F. Burdet, E. Espinosa and R. Guilard, Eur.J.Inorg.Chem. (2005) 1032.
[12] A. Mahammed, I. Goldberg and Z. Gross, Organic Letters, 3 (2001) 3443.
[13] D. A. House, V. McKee and W. T. Robinson, Inorg. Chim. Acta, 160 (1989) 71.
[14] F. Edelmann and U. Behrens, Z. Anorg. Allg. Chem., 432 (1977) 58.
[15] P. L. Gaus, R. M. Benefield, H. Hicsasmaz, B. Perry, J. Villanueva, C. E. Flack, V. B. Pett, S. A. Demoulini, J. C. Faulhaber, D. E. Lynch and J. W. Bacon, Inorg. Chim. Acta, 141 (1988) 61.
[16] V. Vinodu and I. Goldberg, CrystEngComm, 6 (2004) 215.
[17] J. Goodwin, R. Bailey, W. Pennington, R. Rasberry, T. Green, S. Shasho, M. Yongsavanh, V. Echevarria, J. Tiedeken, C. Brown, G. Fromm, S. Lyerly, N. Watson, A. Long and N. De Nitto, Inorg. Chem., 40 (2001) 4217.
[18] J. A. Kaduk and W. R. Scheidt, Inorg. Chem., 13 (1974) 1875.